
Provably Efficient Lottery Ticket Discovery

Cameron R. Wolfe¹†, Qihan Wang¹, Junhyung Lyle Kim¹, and Anastasios Kyriillidis¹

¹Department of Computer Science, Rice University, Houston, TX, USA.

†Corresponding author: Cameron R. Wolfe, crw13@rice.edu.

Abstract

The lottery ticket hypothesis (LTH) [19] claims that randomly-initialized, dense neural networks contain (sparse) subnetworks that, when trained an equal amount in isolation, can match the dense network’s performance. Although LTH is useful for discovering efficient network architectures, its three-step process—pre-training, pruning, and re-training—is computationally expensive, as the dense model must be fully pre-trained. Luckily, “early-bird” tickets can be discovered within neural networks that are minimally pre-trained [67], allowing for the creation of efficient, LTH-inspired training procedures. Yet, no theoretical foundation of this phenomenon exists. We derive an analytical bound for the number of pre-training iterations that must be performed for a winning ticket to be discovered, *thus providing a theoretical understanding of when and why such early-bird tickets exist*. By adopting a greedy forward selection pruning strategy [65], we directly connect the pruned network’s performance to the loss of the dense network from which it was derived, revealing a threshold in the number of pre-training iterations beyond which high-performing subnetworks are guaranteed to exist. We demonstrate the validity of our theoretical results across a variety of architectures and datasets, including multi-layer perceptrons (MLPs) trained on MNIST and several deep convolutional neural network (CNN) architectures trained on CIFAR10 and ImageNet.

1 Introduction

The current trend in deep learning is towards larger models and datasets [6, 11, 14]. Despite the widespread moral and practical questioning of this trend [28, 54, 60, 61], the deep learning community continues to push the limits of experimental scale, finding that severely overparameterized models generalize surprisingly well [49].

In contrast, the proposal of the Lottery Ticket Hypothesis (LTH) [19] has led to significant interest in using pruning techniques to discover small (sometimes sparse) models that perform well. LTH has been explored extensively in practice and was shown to be applicable in even large-scale settings [8, 21, 22, 42, 48, 70, 71]. Such results generally highlight that high-performing subnetworks can be obtained by pruning large, pre-trained models and fine-tuning the pruned weights to convergence (i.e., either from their initial values or some later point) [9, 23, 58].

Although LTH enables the discovery of low-cost architectures, the methodology still requires the presence of a pre-trained, dense model [19, 65], which is expensive to obtain in practice. In particular, LTH follows a three-step procedure of discovering winning tickets, including pre-training, pruning, and re-training, where pre-training is the most costly step [19, 67].

To circumvent the cost of pre-training, several works explore the possibility of pruning networks directly from initialization (i.e., the “strong lottery ticket hypothesis”) [20, 57, 62]. However, subnetworks obtained at initialization cannot yet match the performance of those obtained from fully pre-trained models. Adopting a hybrid approach, recent work has shown that winning tickets can

be obtained from models with minimal pre-training [10, 67] (i.e., “early-bird” tickets). By avoiding the full pre-training cost, such work provides hope that LTH-inspired methodologies could reduce wall-clock training time in comparison to fully training a dense model.

Extensive empirical analysis of LTH has inspired the development of theoretical foundations for winning tickets. Several works have derived bounds for the performance and size of winning tickets in randomly-initialized networks [45, 52, 55]. However, these works require sufficient overparameterization and typically produce sparse networks that do not provably outperform similarly-sized networks trained with stochastic gradient descent (SGD).

Other theoretical works study the performance of winning tickets derived from pre-trained networks by proposing greedy forward selection for pruning MLPs [65, 66]. In addition to enabling convergence analysis of pruned networks, pruning via greedy forward selection was shown to work well for various (deep) network architectures in practice, even on large-scale datasets such as ImageNet [12, 65, 66]. Although some findings from these works apply to randomly-initialized networks given proper assumptions [65], *no work yet exists that determines how different levels of pre-training impact the performance of pruned networks from a theoretical perspective.*

This paper. We propose a novel theoretical framework for analyzing the performance of two-layer neural networks pruned with greedy forward selection [65]. This formulation *i*) accurately reflects the forward selection algorithm used in practice, *ii*) maintains the same rates provided in previous work, and *iii*) is structured such that the loss of the pruned network can be expressed with respect to the loss of the dense model from which it is derived. When combined with SGD convergence bounds for two-layer neural networks [53], this framework can be used to express the loss of a pruned network with respect to the amount of pre-training within the dense model, allowing a theoretical understanding of the early-bird ticket phenomenon to be derived. The key messages of this work are:

- *We obtain a theoretical bound for the amount of pre-training required to discover a winning ticket.* In particular, we show that winning tickets only exist within networks that have surpassed some threshold in the number of pre-training iterations, which exactly reflects observations for early-bird tickets in practice [67].
- We show that this pre-training threshold increases logarithmically with the size of the underlying dataset, offering intuition for why LTH results are difficult to replicate on larger datasets [22, 42].
- To validate our theoretical analysis, we perform extensive experiments across numerous architectures and datasets, including MLPs trained on MNIST [13] and deep CNN architectures trained on CIFAR10 and ImageNet [12, 35]. *We find that the amount of pre-training required to discover high-performing pruned networks consistently increases based on the size of the underlying dataset.*

2 Notation and Preliminaries

Notation. Vectors are represented with bold type (e.g., \mathbf{x}), while scalars are represented by normal type (e.g., x). $\|\cdot\|_2$ represents the ℓ_2 vector norm. Unless otherwise specified, vector norms are always considered to be ℓ_2 norms. $[N]$ is used to represent the set of positive integers from 1 to N (i.e., $[N] = \{1 \dots N\}$). We denote the ball of radius r centered at $\boldsymbol{\mu}$ as $\mathcal{B}(\boldsymbol{\mu}, r)$.

Preliminaries. In addition to basic notation, several relevant constructions are used within our theoretical analysis. We consider two-layer neural networks of width N , defined by (1):

$$f(\mathbf{x}, \Theta) = \frac{1}{N} \sum_{i=1}^N \sigma(\mathbf{x}, \boldsymbol{\theta}_i) \quad (1)$$

where $\Theta = \{\boldsymbol{\theta}_1, \dots, \boldsymbol{\theta}_N\}$ represents all weights within the two-layer neural network. In (1), $\sigma(\cdot, \boldsymbol{\theta}_i)$ represents the activation of a single neuron of the N total neurons in the network:

$$\sigma(\mathbf{x}, \boldsymbol{\theta}_i) = b_i \sigma_+(\mathbf{a}_i^\top \mathbf{x}), \quad (2)$$

where σ_+ is a smooth activation function (e.g., sigmoid or tanh). The majority of our analysis is not dependent upon the choice of activation function; see Section 4. However, it should be noted that the performance of smooth activation functions is comparable to that of non-smooth activations (e.g., ReLU) in practice [47, 65]. The weights of a single neuron are represented by $\boldsymbol{\theta}_i = [b_i, \mathbf{a}_i] \in \mathbb{R}^{d+1}$, where d is the dimension of the input vector.

The training of two-layer networks has recently been shown to be relevant to larger-scale applications and deeper architectures [5, 31, 51]. Additionally, two-layer neural networks have the special property of output activations being separable between neurons. Namely, to produce the network output, (2) is computed for every neuron in the network; then, a uniform average is taken over activations in (1).

We assume that our network is modeling a dataset D , where $|D| = m$. The dataset D has the form $\{\mathbf{x}^{(i)}, y^{(i)}\}_{i=1}^m$, where $\mathbf{x}^{(i)} \in \mathbb{R}^d$ and $y^{(i)} \in \mathbb{R}$ for all $i \in [m]$. In all cases, we consider an ℓ_2 -norm regression loss over this dataset during training:

$$\mathcal{L}[f] = \frac{1}{2} \cdot \mathbb{E}_{(\mathbf{x}, y) \sim D} [(f(\mathbf{x}, \Theta) - y)^2]. \quad (3)$$

We define $\mathbf{y} = [y^{(1)}, y^{(2)}, \dots, y^{(m)}] / \sqrt{m}$. In words, \mathbf{y} represents a concatenated vector of all labels within the dataset D , where each label is divided by a constant factor \sqrt{m} . Similarly, we define $\phi_{i,j} = \sigma(\mathbf{x}^{(j)}, \theta_i)$ as the output of neuron i for the j -th input vector in the dataset. Utilizing this definition, we then construct the vector $\Phi_i = [\phi_{i,1}, \phi_{i,2}, \dots, \phi_{i,m}] / \sqrt{m}$, which is a concatenated vector of output activations for a single neuron across the entire dataset D , again divided by a factor \sqrt{m} . We use \mathcal{M}_N to denote the convex hull over such activation vectors for all N neurons.

$$\mathcal{M}_N = \text{Conv}\{\Phi_i : i \in [N]\}. \quad (4)$$

Here, $\text{Conv}\{\cdot\}$ denotes the convex hull. \mathcal{M}_N forms a marginal polytope of the feature map for all neurons in the two-layer network across every dataset example. We use $\text{Vert}(\mathcal{M}_N)$ to denote the vertices of the marginal polytope \mathcal{M}_N (i.e., $\text{Vert}(\mathcal{M}_N) = \{\Phi_i : i \in [N]\}$). Furthermore, using the construction \mathcal{M}_N , the ℓ_2 loss can be easily defined as follows:

$$\ell(\mathbf{z}) = \frac{1}{2} \|\mathbf{z} - \mathbf{y}\|^2, \quad (5)$$

where $\mathbf{z} \in \mathcal{M}_N$. Finally, we define the diameter of the space \mathcal{M}_N as $\mathcal{D}_{\mathcal{M}_N} = \max_{\mathbf{u}, \mathbf{v} \in \mathcal{M}_N} \|\mathbf{u} - \mathbf{v}\|_2$.

3 From dense to sparse neural networks using greedy forward selection

We assume the existence of a dense, two-layer network of width N , from which the pruned model is constructed. Note that, for now, *no assumption is made regarding the amount of pre-training for the dense model*. Given a subset of neuron indices from the dense model $\mathcal{S} \subseteq [N]$, we denote the output of the pruned subnetwork that only contains this subset of neurons as follows:

$$f_{\mathcal{S}}(\mathbf{x}, \Theta) = \frac{1}{|\mathcal{S}|} \sum_{i \in \mathcal{S}} \sigma(\mathbf{x}, \theta_i). \quad (6)$$

We consider the greedy forward selection approach for pruning, as proposed in [65]. Beginning from an empty network (i.e., $\mathcal{S} = \emptyset$), we aim to discover a subset of neurons $\mathcal{S}^* = \arg \min_{\mathcal{S} \subseteq [N]} \mathcal{L}[f_{\mathcal{S}}]$ such that $|\mathcal{S}^*| \ll N$. Instead of discovering an exact solution to this difficult combinatorial optimization problem, greedy forward selection is used to find an approximate solution. In particular, the pruned network is constructed by greedily selecting the neuron that yields the largest decrease in loss at each iteration. This strategy is described in (7), where k is the number of forward selection steps:

$$\mathcal{S}_{k+1} = \mathcal{S}_k \cup i^*, \quad \text{where } i^* = \arg \min_{i \in [N]} \mathcal{L}[f_{\mathcal{S}_k \cup i}] \quad (7)$$

Using constructions from Section 2, we propose a novel update rule to formalize the greedy selection strategy in (7):

$$\text{(Select new neuron): } \mathbf{q}_k = \arg \min_{\mathbf{q} \in \text{Vert}(\mathcal{M}_n)} \ell\left(\frac{1}{k} \cdot (\mathbf{z}_{k-1} + \mathbf{q})\right) \quad (8)$$

$$\text{(Add neuron to subnetwork): } \mathbf{z}_k = \mathbf{z}_{k-1} + \mathbf{q}_k \quad (9)$$

$$\text{(Uniform average of neuron outputs): } \mathbf{u}_k = \frac{1}{k} \cdot \mathbf{z}_k. \quad (10)$$

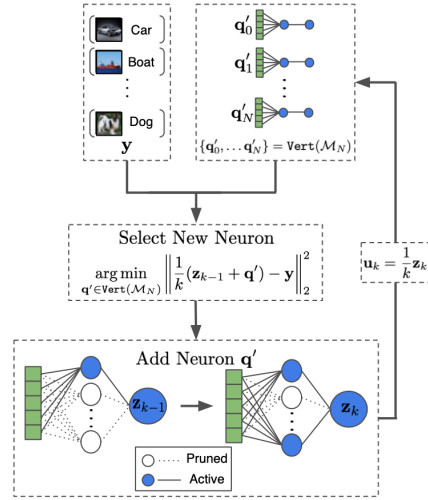


Figure 1: Depiction of the forward selection pruning formulation in (8)-(10).

In words, the recursion in (8)-(10) includes the output of a new neuron, given by \mathbf{q}_k , within the current subnetwork at each pruning iteration based on a greedy minimization of the training loss $\ell(\cdot)$. Then, the output of the pruned subnetwork over the entire dataset at the k -th iteration, given by $\mathbf{u}_k \in \mathcal{M}_N$, is computed by taking a uniform average over the activation vectors of the k active neurons in \mathbf{z}_k , thus exactly matching the formulation in (7). A depiction of this theoretical pruning formulation is provided in Figure 1. Such an exact match between the practical and theoretical pruning formulations is lacking in previous work [65]; see Appendix D. Furthermore, (8)-(10) is structured such that the output of both pruned and dense networks is a uniform average of neuron activations. *Such structure is particularly suited to analyzing the loss of the pruned network with respect to the performance of the network being pruned*, which motivates our proposal of this formulation.

4 How much pre-training do we really need?

As previously stated, no existing theoretical analysis has quantified the impact of pre-training on the performance of a pruned subnetwork. Here, we solve this problem by extending existing LTH theory to determine the relationship between pre-training and the discovery of winning tickets. We find that winning tickets only exist in dense models that surpass a threshold in the number of pre-training iterations, which is dependent on the size of the underlying dataset. Full proofs are deferred to Appendix A, but we provide a sketch of the analysis within this section. We first derive a convergence rate for our pruning formulation in (8)-(10), expressed with respect to k (i.e., the size of the pruned model).

Theorem 1. *The following expression for the objective loss is true for iterates derived after k iterations of the update rule in (8)-(10) with a two-layer network of width N :*

$$\ell(\mathbf{u}_k) \leq \frac{1}{k} \left(\ell(\mathbf{u}_1) - \mathcal{L}_N + \frac{1}{2} \mathcal{D}_{\mathcal{M}_N}^2 \right) + \mathcal{L}_N \approx \mathcal{O} \left(\frac{1}{k} \right) + \mathcal{L}_N. \quad (11)$$

Here, \mathcal{L}_N represents the loss achieved by the dense network.

One can trivially observe from Theorem 1 that the loss will only decrease during successive pruning iterations if \mathcal{L}_N does not dominate the expression in (11), thus raising the question: *How can we ensure \mathcal{L}_N is small enough for the pruned network to perform well?* To answer this question, we draw upon convergence analysis for two-layer neural networks trained with stochastic gradient descent (SGD) [53]. We first make the following assumption.

Assumption 1. *For some constant $\delta \in \mathbb{R}$, we assume the first and second derivatives of the network’s activation function are bounded, such that $|\sigma'_+(\cdot)| \leq \delta$ and $|\sigma''_+(\cdot)| \leq \delta$ for σ_+ defined in (2).*

Given this assumption, we can use the analysis of [53] to unroll the value of \mathcal{L}_N in (11) and determine how much pre-training is required for the pruned network to perform well.

Theorem 2. *Assume that Assumption 1 holds and that a two-layer neural network of width N was trained for t iterations with SGD over a dataset D of size m . Additionally, assume that $Nd > m^2$ and $m > d$, where d represents the input dimension of data in D . Let Θ_t represent the parameters of the dense network after t iterations. When the dense network is pruned via (8)-(10) for k iterations, it is guaranteed to achieve a loss given by $\mathcal{L}' \propto \mathcal{O}(\frac{1}{k})$, if t satisfies the following condition:*

$$t \gtrsim \mathcal{O} \left(\frac{-\log(k)}{\log(1 - c\frac{d}{m^2})} \right), \quad \text{where } c \text{ is a positive constant.} \quad (12)$$

Otherwise, the loss of the pruned network may not improve over successive iterations of (8)-(10).

In words, this theorem states that *a threshold exists in the number of pre-training iterations of a dense network, beyond which high-performing subnetworks are guaranteed to exist*. Denoting this threshold as t^* , in the case that $m^2 \gg d$, $\lim_{m \rightarrow \infty} t^* = \infty$, implying that larger datasets require more pre-training. Similarly, when $m^2 \approx d$, $\lim_{m \rightarrow cd} t^* = 0$, demonstrating that minimal pre-training is required to discover winning tickets on smaller datasets. Interestingly, t^* scales logarithmically with the size of the dataset, due to the logarithm in the denominator of (12), implying that the amount of required pre-training will plateau as the underlying dataset becomes increasingly large. A similar result can also be derived using gradient descent (GD) instead of SGD; see Appendix A.

In addition to enabling the above analysis, our pruning formulation in (8)-(10) achieves a faster convergence rate given proper assumptions.

Theorem 3. Assume that $\mathcal{B}(\mathbf{y}, \gamma) \in \mathcal{M}_N$. Then, the following bound is achieved for two-layer neural networks of width N after k iterations of (8)-(10):

$$\ell(\mathbf{u}_k) = \mathcal{O}\left(\frac{1}{k^2 \min(1, \gamma)}\right), \quad \text{where } \gamma \text{ is a positive constant.}$$

Discussion. Despite using a more realistic update rule, our $\mathcal{O}(\frac{1}{k})$ rate in Theorem 2 matches that of previous work [65] and removes smoothness assumptions on the data and activation function. Furthermore, in Theorem 3, we prove that (8)-(10) can achieve a faster rate of $\mathcal{O}(\frac{1}{k^2})$ given that $\mathcal{B}(\mathbf{y}, \gamma) \in \mathcal{M}_N^1$, again eliminating the smoothness assumptions adopted in previous work. Therefore, our pruning formulation *i*) reflects the practical pruning algorithm and *ii*) recovers the convergence rates reported in previous work under milder assumptions [65]. As such, we posit that (8)-(10) is a generally useful formulation for the theoretical analysis of pruning via greedy forward selection.

Including \mathcal{L}_N in (11) allows subnetwork performance to be connected to the amount of pre-training performed on the dense network. This connection leads to the discovery of a pre-training threshold beyond which winning tickets must exist, which exactly matches experimental observations of early-bird tickets [67]. While previous work focuses on discovering early-bird tickets without providing any *a priori* understanding of how much pre-training will be needed, our finding provides insight regarding when and why such early-bird tickets exist. Furthermore, the finding that larger datasets require the dense model to be pre-trained more for high-performing subnetworks to be discovered provides insight into the difficulty of applying LTH to larger-scale datasets [21, 22, 42].

It should be noted that our results specifically focus on the training loss of the dense network and subnetwork. In practice, the ability of a subnetwork to generalize well to some test set would be a more realistic criterion for the discovery of a winning ticket. We conjecture that our analysis can be extended to achieve bounds on subnetwork test accuracy by leveraging existing theory on the generalization performance of neural networks [2, 37]. We leave such analysis as future work.

Proof Sketches. We now provide brief sketches of the theoretical results within this section. Our analysis begins by deriving an analytical expression for $\ell(\mathbf{u}_k)$ with respect to \mathcal{L}_N —the loss of the dense network; see Theorem 1. We derive the expression for $\ell(\mathbf{u}_k)$ as follows:

- By invoking our technical lemmas and the definition of $\mathcal{D}_{\mathcal{M}_N}$, we start at proving the bound: $\ell(\mathbf{u}_k) = \min_{\mathbf{q} \in \text{Vert}(\mathcal{M}_N)} \ell(\frac{1}{k}(\mathbf{z}_{k-1} + \mathbf{q})) \leq \ell(\mathbf{u}_{k-1}) + \frac{1}{k} \langle \nabla \ell(\mathbf{u}_{k-1}), \mathbf{s}_k - \mathbf{u}_{k-1} \rangle + \frac{1}{k^2} \cdot \mathcal{D}_{\mathcal{M}_N}^2$. To prove this bound, we derive *i*) a bound on the value of $\ell(\mathbf{s})$ for $\mathbf{s} \in \mathcal{M}_N$ and *ii*) an inequality for $(\mathbf{u}_k - \mathbf{u}_{k-1})$ where $\mathbf{u}_k, \mathbf{u}_{k-1} \in \mathcal{M}_N$ are adjacent iterates of (8)-(10).
- We then observe that $\mathcal{L}_N \geq \ell(\mathbf{u}_{k-1}) + \langle \nabla \ell(\mathbf{u}_{k-1}), \mathbf{s}_k - \mathbf{u}_{k-1} \rangle$, which yields $\ell(\mathbf{u}_k) - \mathcal{L}_N - \frac{1}{k} \cdot \mathcal{D}_{\mathcal{M}_N}^2 \leq (1 - \frac{1}{k}) \cdot (\ell(\mathbf{u}_{k-1}) - \mathcal{L}_N - \frac{1}{k} \cdot \mathcal{D}_{\mathcal{M}_N}^2)$.
- By unrolling the above recursion over k iterations, we derive the expression in Theorem 1 showing that $\ell(\mathbf{u}_k) \leq \mathcal{O}(\frac{1}{k}) + \mathcal{L}_N$.

From here, we draw upon convergence bounds for two-layer neural networks trained with SGD [53] to unroll the value of \mathcal{L}_N within Theorem 1.² By connecting our previous pruning rate with the convergence rate for the two-layer neural network, we can express the loss of the pruned network with respect to the number of SGD pre-training iterations. This analysis, which is summarized in Theorem 2, follows the steps shown below.

- By taking the expectation over $\ell(\mathbf{u}_k)$, we derive the following:

$$\mathbb{E}[\ell(\mathbf{u}_k)] \leq \frac{1}{k} \mathbb{E}[\ell(\mathbf{u}_1)] + \frac{1}{2k} \mathbb{E}[\mathcal{D}_{\mathcal{M}_N}^2] + \frac{(k-1)\zeta}{2mk} \left(1 - c \frac{d}{m^2}\right)^t \mathcal{L}_0,$$

where $\mathcal{L}_0 = \|f(\mathbf{X}, \Theta_0) - \mathbf{Y}\|_2^2$ and $\zeta = \left[\max\left(\kappa, \left(1 - c_1 \left(c_2 \sqrt{\frac{m}{d}}\right)^{\frac{1}{N^a}}\right)\right)\right]^{-1}$. This bound is obtained by invoking Theorem 2.6 from [7] and leveraging the independence of expectations to derive a bound for the value of $\mathbb{E}[\|f(\mathbf{X}, \Theta_t) - \mathbf{Y}\|_2^2]$.

¹We demonstrate that this assumption is mild in practice by performing extensive analysis using two-layer neural networks trained on numerous image classification datasets, revealing that $\mathcal{B}(\mathbf{y}, \gamma) \in \mathcal{M}_N$ is often true, even with minimal pre-training; see Appendix B.

²In order for the Theorems in [53] to be applicable, overparameterization assumptions on the two-layer neural network must be satisfied, given by $Nd > m^2$ and $m > d$. Additionally, we must adopt Assumption 1.

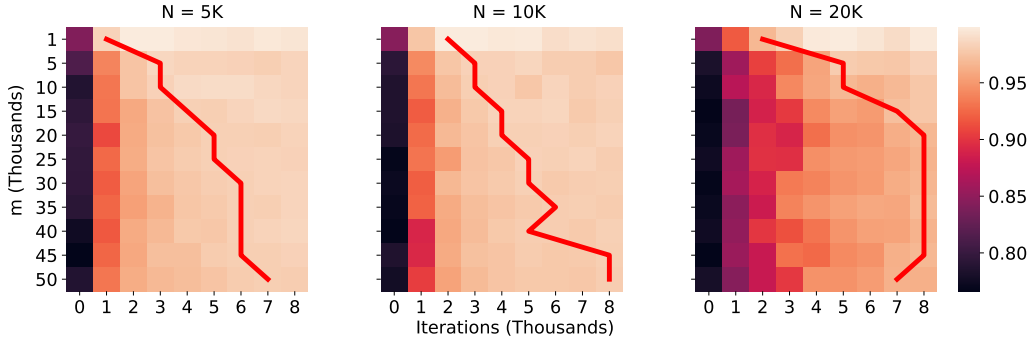


Figure 2: Accuracies of pruned MLP models on MNIST. Different sub-plots represent different numbers of hidden nodes within the dense model. Different sub-dataset sizes are depicted in the y-axis. As seen in the x-axis, models are trained for 8K iterations and pruned to a hidden dimension of 200 every 1K iterations to measure subnetwork performance. Color represents accuracy over the entire training dataset. Pruned models are not fine-tuned. The red line depicts for each sub-dataset the point at which subnetworks surpass the performance of the best pruned model on the full dataset.

- To cancel the term of $k - 1$ within the numerator of the above expression, we realize that the value of t must be increased such that $(1 - c \frac{d}{m^2})^t \approx \mathcal{O}(\frac{1}{k})$. After noticing that any value of t beyond this approximate value would also lead to a good pruning loss, we obtain the pre-training bound stated in Theorem 6.

We also show that our pruning formulation achieves an accelerated $\mathcal{O}(\frac{1}{k^2})$ rate under the assumption that $\mathcal{B}(\mathbf{y}, \gamma) \in \mathcal{M}_N$. Because this proof is more technically involved, we defer it to Appendix A.

5 Related Work

Many variants have been proposed for both structured [25, 36, 41, 65] and unstructured [16, 17, 19, 26] pruning. Generally, structured pruning, which prunes entire channels or neurons of a network instead of individual weights, is considered more practical, as it can achieve speedups without leveraging specialized libraries for sparse computation. Existing pruning criterion include the norm of weights [36, 41, 72], feature reconstruction error [30, 44, 66, 68], or even gradient-based sensitivity measures [4, 63, 72]. While most pruning methodologies perform backward elimination of neurons within the network [19, 21, 41, 42, 68], some recent research has focused on forward selection structured pruning strategies [65, 66, 72]. We adopt greedy forward selection within this work, as it has been previously shown to yield superior performance in comparison to greedy backward elimination [65].

Our analysis resembles that of the Frank-Wolfe algorithm [18, 34], a widely-used technique for constrained, convex optimization. Recent work has shown that training deep networks with Frank-Wolfe can be made feasible in certain cases despite the non-convex nature of neural network training [3, 56]. Instead of training networks from scratch with Frank-Wolfe, however, we use a Frank-Wolfe-style approach to greedily select neurons from a pre-trained model. Such a formulation casts structured pruning as convex optimization over a marginal polytope, which can be analyzed similarly to Frank-Wolfe [65, 66] and loosely approximates networks trained with standard, gradient-based techniques [65]. Alternative methods of analysis for greedy selection algorithms could also be constructed with the use of sub-modular optimization techniques [50].

Much work has been done to analyze the convergence properties of neural networks trained with gradient-based techniques [7, 27, 32, 69]. Such convergence rates were originally explored for wide, two-layer neural networks using mean-field analysis techniques [46, 47]. Similar techniques were later used to extend such analysis to deeper models [43, 64]. Generally, recent work on neural network training analysis has led to novel analysis techniques [27, 32], extensions to alternate optimization methodologies [33, 53], and even generalizations to different architectural components [24, 39, 69]. By adopting and extending such analysis, we aim to bridge the gap between the theoretical understanding of neural network training and LTH.

6 Experiments

In this section, we empirically validate our theoretical results from Section 4, which predict that larger datasets require more pre-training for winning tickets to be discovered. The pruning strategy in (7) has already been empirically analyzed in previous work [65]. Therefore, we *differentiate our experiments by providing an in-depth analysis of the scaling properties of (7) with respect to the size and complexity of the underlying dataset*. In particular, we produce synthetic “sub-datasets” of different sizes and measure the amount of pre-training required to discover a winning ticket on each, thus providing a more thorough understanding of how pre-training costs can be minimized within LTH. See Figure 3 for a high-level illustration of our experimental process. We perform analysis with MLPs on MNIST [13] and with deep CNNs (i.e., ResNet34 [29] and MobileNetV2 [59]) on CIFAR10 and ImageNet [12, 35]. We find that *i) winning tickets can be consistently discovered without incurring the full pre-training cost, and ii) the amount of pre-training required to discover a winning ticket increases with the size and complexity of the underlying dataset in practice*. All experiments are run on an internal cluster with two Nvidia RTX 3090 GPUs.

MLP Experiments. We perform structured pruning experiments with two-layer MLP models on MNIST³ [13] by pruning hidden neurons via greedy forward selection. To match the single output neuron setup described in Section 2, we binarize MNIST labels by considering all labels less than five as zero and vice versa. Our model architecture matches the description in Section 2 with a few minor differences. Namely, we adopt a ReLU hidden activation and apply a sigmoid output transformation to enable training with binary cross entropy loss. Experiments are conducted with several different hidden dimensions (i.e., $N \in \{5K, 10K, 20K\}$). We pre-train the MLP with an SGD optimizer, momentum of 0.9, no weight decay, and a batch size of 128, which we found to perform well in multiple different experimental settings. Further hyperparameter choices (e.g., learning rate, size of pruned model, and number of training iterations) are explained in Appendix C.1.

To study how dataset size impacts the discovery of early-bird tickets, we construct sub-datasets of sizes 1K to 50K (i.e., in increments of 5K) from the original MNIST dataset by randomly sampling an equal number of examples from each of the 10 original classes. The MLP is pre-trained for 8K iterations in total and pruned every 1K iterations to a size of 200 hidden nodes; see Appendix C.1 for a precise, algorithmic description of the MLP pruning process. After pruning, the accuracy of the pruned model over the entire training dataset is recorded (i.e., no fine-tuning is performed), allowing the impact of dataset size and pre-training length on subnetwork performance to be observed. See Figure 2 for these results, which are averaged across three trials.

The performance of pruned subnetworks in Figure 2 matches the theoretical analysis provided in Section 4 for all different sizes of MLPs. Namely, *as the dataset size increases, so does the amount of pre-training required to produce a high-performing subnetwork*. To see this, one can track the trajectory of the red line, which traces the point at which the accuracy of the best performing subnetwork for the full dataset is surpassed at each sub-dataset size. This trajectory clearly illustrates that pre-training requirements for winning tickets increase with the size of the dataset. Furthermore, this increase in the amount of required pre-training is seemingly logarithmic, as the trajectory typically plateaus at larger dataset sizes.

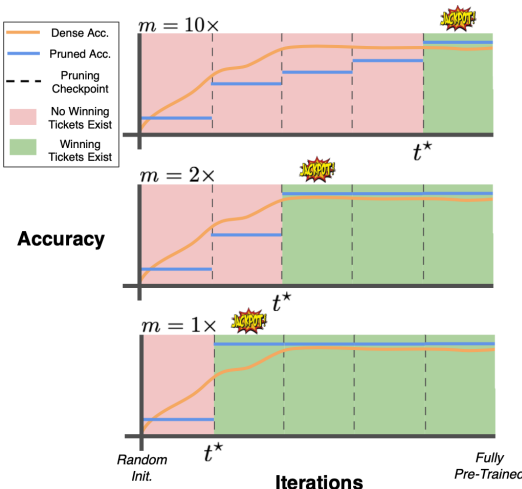


Figure 3: Our experimental process. Models are fully pre-trained for different sub-dataset sizes. At several intermediate points during training, the model is pruned to determine if a winning ticket can be discovered.

³Images are flattened before being passed as input to the MLP. No data augmentation is used.

| Model | Dataset Size | Pruned Accuracy | | | | Dense Accuracy |
|-------------|--------------|-----------------|---------|---------|---------|----------------|
| | | 20K It. | 40K It. | 60K It. | 80K It. | |
| MobileNetV2 | 10K | 82.32 | 86.18 | 86.11 | 86.09 | 83.13 |
| | 30K | 80.19 | 87.79 | 88.38 | 88.67 | 87.62 |
| | 50K | 86.71 | 88.33 | 91.79 | 91.77 | 91.44 |
| ResNet34 | 10K | 75.29 | 85.47 | 85.56 | 85.01 | 86.74 |
| | 30K | 84.06 | 91.59 | 92.31 | 92.15 | 92.14 |
| | 50K | 89.79 | 91.34 | 94.28 | 94.23 | 94.18 |

Table 1: CIFAR10 test accuracy for subnetworks derived from dense networks with varying pre-training amounts (i.e., number of training iterations listed in top row) and sub-dataset sizes.

Interestingly, despite the use of a small-scale dataset, high-performing subnetworks are never discovered at initialization, revealing that some minimal amount of pre-training is often required to discover winning tickets via greedy forward selection even with very small datasets. Previous work claims that winning tickets may exist at initialization in theory [65]. In contrast, our empirical analysis shows that this is not the case even in simple experimental settings.

CNN Experiments. We perform structured pruning experiments (i.e., channel-based pruning) using ResNet34 [29] and MobileNetV2 [59] architectures on CIFAR10 and ImageNet [12, 35]. We adopt the same generalization of greedy forward selection to pruning deep networks as described in [65]. More specifically, structured pruning of CNN channels is performed layer-by-layer using the same greedy forward selection strategy described in (7). At each layer, we define a stopping criterion ϵ based on the maximum deviation between subnetwork and dense network loss. A complete description of the algorithm used for greedy forward selection on deep CNN architectures is provided in Appendix C.2. We follow the three-stage methodology—pre-training, pruning, and fine-tuning—and modify both the size of the underlying dataset and the amount of pre-training to examine their impact on subnetwork performance. Standard data augmentation and splits are adopted for both datasets.

CIFAR10. Three different CIFAR10 sub-datasets are created with 10K, 30K, and 50K (i.e., full dataset) examples by randomly and uniformly sampling examples from each of the ten classes. Pre-training is conducted for 80K iterations (i.e., 200 epochs for the full dataset) using SGD with momentum and a cosine learning rate decay schedule starting at 0.1. We use a batch size of 128 and weight decay of $5 \cdot 10^{-4}$.⁴ Model checkpoints are saved every 20K iterations so that winning tickets can be discovered within dense models with different amounts of pre-training. Before measuring test accuracy, subnetworks are fine-tuned for 2500 iterations (i.e., 50 epochs for the full dataset) on their respective sub-datasets using cosine learning rate decay. For MobileNetV2, we use $\epsilon = 0.02$ and an initial learning rate of 0.01 for fine-tuning, while for ResNet34 we use $\epsilon = 0.05$ and an initial learning rate of 0.01.⁵ These settings for ϵ yield subnetworks with a 40% decrease in FLOPS and 20% decrease in model parameters in comparison to the dense model. We ensure subnetworks utilize a consistent number of FLOPS and parameters across all experimental settings.

The results of these experiments are presented in Table 1. The amount of training required to discover a winning ticket consistently increases with the size of the dataset. For example, with MobileNetV2, a winning ticket is discovered on the 10K sub-dataset in only 40K iterations, while for the 30K and 50K sub-datasets, winning tickets are not discovered until 60K iterations of pre-training have been completed. A nearly identical pattern is observed when experiments are replicated with the ResNet34 architecture. Furthermore, we observe that the performance of winning tickets often surpasses the performance of the fully-trained dense network *without completing the full pre-training procedure*. For example, the pruned MobileNetV2 on the 10K sub-dataset exceeds the performance of the dense model by over 3% after only 40K pre-training iterations, while the pruned ResNet34 on the full CIFAR10 dataset exceeds dense network performance with only 60K iterations of pre-training.

ImageNet. We perform pruning experiments on the ILSVRC2012, 1000-class dataset [12]. The goal of these experiments is to determine whether early-bird tickets exist for models pruned to different FLOP levels.⁶ Adopting the settings of [65], models are pre-trained for 150 epochs in total using

⁴Our pre-training settings are adopted from a popular repository for the CIFAR10 dataset [40].

⁵These settings are derived using a grid search over values of ϵ and the learning rate; see Appendix C.2.

⁶We do not experiment with different sub-dataset sizes on ImageNet due to limited computational resources.

| Model | FLOP (Param) Ratio | Pruned Accuracy | | | Dense Accuracy |
|-------------|-----------------------|-----------------|-----------|-----------|----------------|
| | | 50 Epoch | 100 Epoch | 150 Epoch | |
| MobileNetV2 | 60% (80%) | 70.05 | 71.14 | 71.53 | 71.70 |
| | 40% (65%) | 69.23 | 70.36 | 71.10 | |
| ResNet34 | 60% (80%) | 71.68 | 72.56 | 72.65 | 73.20 |
| | 40% (65%) | 69.87 | 71.44 | 71.33 | |

Table 2: Test accuracy on ImageNet of subnetworks with different FLOP levels derived from dense models with varying amounts of pre-training (i.e., training epochs listed in top row). We report the FLOP/parameter ratio after pruning with respect to the FLOPS/parameters of the dense model.

SGD with momentum and cosine learning rate decay with an initial learning rate of 0.1. We use a batch size of 128 and weight decay of $5 \cdot 10^{-4}$. Model checkpoints are saved every 50 epochs so that subnetwork testing accuracy can be measured with different levels of pre-training. Models are pruned using two different values of ϵ for each architecture. Namely, we first prune models with $\epsilon = 0.02$ and $\epsilon = 0.05$ for MobileNetV2 and ResNet34, respectively, yielding subnetworks with a 40% reduction in FLOPS and 20% reduction in parameters in comparison to the dense model. Then, the value of ϵ is slightly increased (i.e., $\epsilon = 0.05$ and $\epsilon = 0.08$ for MobileNetV2 and ResNet34, respectively) to yield smaller subnetworks with a 60% reduction in FLOPS and 35% reduction in model parameters in comparison to the dense model. All sub-networks are fine-tuned for 80 epochs using SGD and cosine learning rate decay with an initial learning rate of 0.01, which we find to perform consistently well across experimental settings.

The results of these experiments are reported in Table 2. As can be seen, for both FLOP levels, the test accuracy of subnetworks after pruning and reaches a plateau without completing the entire pre-training procedure. Namely, although the dense network is pre-trained for 150 epochs, winning tickets can be discovered after only 100 epochs of pre-training. Such a trend is true for both levels of pruning that were tested (i.e., 60% and 40% of FLOPS). Furthermore, subnetworks with only 50 epochs of pre-training still perform well in many cases in comparison to subnetworks with more pre-training. For example, the 60% FLOPS ResNet34 subnetwork with 50 epochs of pre-training achieves a testing accuracy within 1% of the pruned model derived from the fully pre-trained network. In other words, although more pre-training may lead to slightly improved subnetwork performance in certain cases, *high-performing subnetworks can often be discovered with minimal pre-training even on large-scale datasets like ImageNet*, resulting in drastic computational savings.

Interestingly, discovering a winning ticket on the ImageNet dataset takes roughly 500K pre-training iterations (i.e., 100 epochs). In comparison, discovering winning tickets on the MNIST and CIFAR10 datasets takes roughly 8K and 60K iterations, respectively, *revealing that pre-training requirements are dependent upon dataset size and complexity even across drastically different experimental settings*.

7 Conclusion

Our work provides a theoretical understanding of the early-bird ticket phenomenon. By extending existing analysis of pruning via greedy forward selection [65] and connecting subnetwork performance to SGD training dynamics [53], *we derive a closed-form expression for the loss of a pruned network with respect to the loss of the dense model from which it is derived*. Leveraging this analysis, we discover a threshold in the number of pre-training iterations for the dense model, dependent on the size of the underlying dataset, beyond which winning tickets are guaranteed to exist. Such a threshold exactly matches empirical observations of early-bird tickets and provides intuition for why LTH is difficult to replicate on large-scale datasets. We empirically verify our theoretical findings over several datasets (i.e., MNIST, CIFAR10, and ImageNet) with numerous network architectures (i.e., MLP, MobileNetV2, and ResNet34), showing that the amount of pre-training required to discover a winning ticket is consistently dependent on the size of the underlying dataset. Several open problems remain, such as extending our analysis beyond two-layer networks and deriving generalization bounds for subnetworks pruned with greedy forward selection. We hope that our work sparks further interest in the area so that a better theoretical understanding of LTH can be achieved.

References

- [1] Zeyuan Allen-Zhu, Yuanzhi Li, and Yingyu Liang. Learning and generalization in overparameterized neural networks, going beyond two layers. *arXiv preprint arXiv:1811.04918*, 2018.
- [2] Sanjeev Arora, Simon Du, Wei Hu, Zhiyuan Li, and Ruosong Wang. Fine-grained analysis of optimization and generalization for overparameterized two-layer neural networks. In *International Conference on Machine Learning*, pages 322–332. PMLR, 2019.
- [3] Francis Bach. Breaking the Curse of Dimensionality with Convex Neural Networks. *arXiv e-prints*, page arXiv:1412.8690, December 2014.
- [4] Cenk Baykal, Lucas Liebenwein, Igor Gilitschenski, Dan Feldman, and Daniela Rus. SiPPing Neural Networks: Sensitivity-informed Provable Pruning of Neural Networks. *arXiv e-prints*, page arXiv:1910.05422, October 2019.
- [5] Eugene Belilovsky, Michael Eickenberg, and Edouard Oyallon. Greedy layerwise learning can scale to imagenet. In *International conference on machine learning*, pages 583–593. PMLR, 2019.
- [6] Tom B. Brown, Benjamin Mann, Nick Ryder, Melanie Subbiah, Jared Kaplan, Prafulla Dhariwal, Arvind Neelakantan, Pranav Shyam, Girish Sastry, Amanda Askell, Sandhini Agarwal, Ariel Herbert-Voss, Gretchen Krueger, Tom Henighan, Rewon Child, Aditya Ramesh, Daniel M. Ziegler, Jeffrey Wu, Clemens Winter, Christopher Hesse, Mark Chen, Eric Sigler, Mateusz Litwin, Scott Gray, Benjamin Chess, Jack Clark, Christopher Berner, Sam McCandlish, Alec Radford, Ilya Sutskever, and Dario Amodei. Language Models are Few-Shot Learners. *arXiv e-prints*, page arXiv:2005.14165, May 2020.
- [7] Xiangyu Chang, Yingcong Li, Samet Oymak, and Christos Thrampoulidis. Provable benefits of overparameterization in model compression: From double descent to pruning neural networks. *arXiv preprint arXiv:2012.08749*, 2020.
- [8] Tianlong Chen, Jonathan Frankle, Shiyu Chang, Sijia Liu, Yang Zhang, Michael Carbin, and Zhangyang Wang. The lottery tickets hypothesis for supervised and self-supervised pre-training in computer vision models. *arXiv preprint arXiv:2012.06908*, 2020.
- [9] Tianlong Chen, Jonathan Frankle, Shiyu Chang, Sijia Liu, Yang Zhang, Zhangyang Wang, and Michael Carbin. The Lottery Ticket Hypothesis for Pre-trained BERT Networks. *arXiv e-prints*, page arXiv:2007.12223, July 2020.
- [10] Xiaohan Chen, Yu Cheng, Shuohang Wang, Zhe Gan, Zhangyang Wang, and Jingjing Liu. EarlyBERT: Efficient BERT Training via Early-bird Lottery Tickets. *arXiv e-prints*, page arXiv:2101.00063, December 2020.
- [11] Alexis Conneau, Kartikay Khandelwal, Naman Goyal, Vishrav Chaudhary, Guillaume Wenzek, Francisco Guzmán, Edouard Grave, Myle Ott, Luke Zettlemoyer, and Veselin Stoyanov. Unsupervised Cross-lingual Representation Learning at Scale. *arXiv e-prints*, page arXiv:1911.02116, November 2019.
- [12] Jia Deng, Wei Dong, Richard Socher, Li-Jia Li, Kai Li, and Li Fei-Fei. Imagenet: A large-scale hierarchical image database. In *2009 IEEE conference on computer vision and pattern recognition*, pages 248–255. Ieee, 2009.
- [13] Li Deng. The mnist database of handwritten digit images for machine learning research. *IEEE Signal Processing Magazine*, 29(6):141–142, 2012.
- [14] Alexey Dosovitskiy, Lucas Beyer, Alexander Kolesnikov, Dirk Weissenborn, Xiaohua Zhai, Thomas Unterthiner, Mostafa Dehghani, Matthias Minderer, Georg Heigold, Sylvain Gelly, Jakob Uszkoreit, and Neil Houlsby. An Image is Worth 16x16 Words: Transformers for Image Recognition at Scale. *arXiv e-prints*, page arXiv:2010.11929, October 2020.
- [15] Simon Du, Jason Lee, Haochuan Li, Liwei Wang, and Xiyu Zhai. Gradient descent finds global minima of deep neural networks. In *International Conference on Machine Learning*, pages 1675–1685. PMLR, 2019.
- [16] Utku Evci, Trevor Gale, Jacob Menick, Pablo Samuel Castro, and Erich Elsen. Rigging the Lottery: Making All Tickets Winners. *arXiv e-prints*, page arXiv:1911.11134, November 2019.

- [17] Utku Evci, Yani A. Ioannou, Cem Keskin, and Yann Dauphin. Gradient Flow in Sparse Neural Networks and How Lottery Tickets Win. *arXiv e-prints*, page arXiv:2010.03533, October 2020.
- [18] Marguerite Frank, Philip Wolfe, et al. An algorithm for quadratic programming. *Naval research logistics quarterly*, 3(1-2):95–110, 1956.
- [19] Jonathan Frankle and Michael Carbin. The Lottery Ticket Hypothesis: Finding Sparse, Trainable Neural Networks. *arXiv e-prints*, page arXiv:1803.03635, March 2018.
- [20] Jonathan Frankle, Gintare Karolina Dziugaite, Daniel M Roy, and Michael Carbin. Pruning neural networks at initialization: Why are we missing the mark? *arXiv preprint arXiv:2009.08576*, 2020.
- [21] Jonathan Frankle, Gintare Karolina Dziugaite, Daniel M. Roy, and Michael Carbin. Stabilizing the Lottery Ticket Hypothesis. *arXiv e-prints*, page arXiv:1903.01611, March 2019.
- [22] Trevor Gale, Erich Elsen, and Sara Hooker. The State of Sparsity in Deep Neural Networks. *arXiv e-prints*, page arXiv:1902.09574, February 2019.
- [23] Sharath Girish, Shishira R. Maiya, Kamal Gupta, Hao Chen, Larry Davis, and Abhinav Shrivastava. The Lottery Ticket Hypothesis for Object Recognition. *arXiv e-prints*, page arXiv:2012.04643, December 2020.
- [24] Surbhi Goel, Adam Klivans, and Raghu Meka. Learning One Convolutional Layer with Overlapping Patches. *arXiv e-prints*, page arXiv:1802.02547, February 2018.
- [25] Song Han, Xingyu Liu, Huizi Mao, Jing Pu, Ardavan Pedram, Mark A. Horowitz, and William J. Dally. EIE: Efficient Inference Engine on Compressed Deep Neural Network. *arXiv e-prints*, page arXiv:1602.01528, February 2016.
- [26] Song Han, Huizi Mao, and William J. Dally. Deep Compression: Compressing Deep Neural Networks with Pruning, Trained Quantization and Huffman Coding. *arXiv e-prints*, page arXiv:1510.00149, October 2015.
- [27] Boris Hanin and Mihai Nica. Finite depth and width corrections to the neural tangent kernel. *arXiv preprint arXiv:1909.05989*, 2019.
- [28] Karen Hao. Training a single ai model can emit as much carbon as five cars in their lifetimes, June 2019.
- [29] Kaiming He, Xiangyu Zhang, Shaoqing Ren, and Jian Sun. Deep Residual Learning for Image Recognition. *arXiv e-prints*, page arXiv:1512.03385, December 2015.
- [30] Yihui He, Xiangyu Zhang, and Jian Sun. Channel Pruning for Accelerating Very Deep Neural Networks. *arXiv e-prints*, page arXiv:1707.06168, July 2017.
- [31] Chris Hettinger, Tanner Christensen, Ben Ehler, Jeffrey Humpherys, Tyler Jarvis, and Sean Wade. Forward thinking: Building and training neural networks one layer at a time. *arXiv preprint arXiv:1706.02480*, 2017.
- [32] Arthur Jacot, Franck Gabriel, and Clément Hongler. Neural tangent kernel: Convergence and generalization in neural networks. *arXiv preprint arXiv:1806.07572*, 2018.
- [33] Gauri Jagatap and Chinmay Hegde. Learning relu networks via alternating minimization. *arXiv preprint arXiv:1806.07863*, 2018.
- [34] Martin Jaggi. Revisiting Frank-Wolfe: Projection-free sparse convex optimization. In Sanjoy Dasgupta and David McAllester, editors, *Proceedings of the 30th International Conference on Machine Learning*, volume 28 of *Proceedings of Machine Learning Research*, pages 427–435, Atlanta, Georgia, USA, 17–19 Jun 2013. PMLR.
- [35] Alex Krizhevsky, Geoffrey Hinton, et al. Learning multiple layers of features from tiny images. 2009.
- [36] Hao Li, Asim Kadav, Igor Durdanovic, Hanan Samet, and Hans Peter Graf. Pruning Filters for Efficient ConvNets. *arXiv e-prints*, page arXiv:1608.08710, August 2016.
- [37] Xingguo Li, Junwei Lu, Zhaoran Wang, Jarvis Haupt, and Tuo Zhao. On tighter generalization bound for deep neural networks: Cnns, resnets, and beyond. *arXiv preprint arXiv:1806.05159*, 2018.
- [38] Yuanzhi Li and Yingyu Liang. Learning overparameterized neural networks via stochastic gradient descent on structured data. *arXiv preprint arXiv:1808.01204*, 2018.

- [39] Yuanzhi Li and Yang Yuan. Convergence Analysis of Two-layer Neural Networks with ReLU Activation. *arXiv e-prints*, page arXiv:1705.09886, May 2017.
- [40] Kuang Liu. Pytorch-cifar. <https://github.com/kuangliu/pytorch-cifar>, 2017.
- [41] Zhuang Liu, Jianguo Li, Zhiqiang Shen, Gao Huang, Shoumeng Yan, and Changshui Zhang. Learning Efficient Convolutional Networks through Network Slimming. *arXiv e-prints*, page arXiv:1708.06519, August 2017.
- [42] Zhuang Liu, Mingjie Sun, Tinghui Zhou, Gao Huang, and Trevor Darrell. Rethinking the Value of Network Pruning. *arXiv e-prints*, page arXiv:1810.05270, October 2018.
- [43] Yiping Lu, Chao Ma, Yulong Lu, Jianfeng Lu, and Lexing Ying. A Mean-field Analysis of Deep ResNet and Beyond: Towards Provable Optimization Via Overparameterization From Depth. *arXiv e-prints*, page arXiv:2003.05508, March 2020.
- [44] Jian-Hao Luo, Jianxin Wu, and Weiyao Lin. ThiNet: A Filter Level Pruning Method for Deep Neural Network Compression. *arXiv e-prints*, page arXiv:1707.06342, July 2017.
- [45] Eran Malach, Gilad Yehudai, Shai Shalev-Shwartz, and Ohad Shamir. Proving the Lottery Ticket Hypothesis: Pruning is All You Need. *arXiv e-prints*, page arXiv:2002.00585, February 2020.
- [46] Song Mei, Theodor Misiakiewicz, and Andrea Montanari. Mean-field theory of two-layers neural networks: dimension-free bounds and kernel limit. *arXiv e-prints*, page arXiv:1902.06015, February 2019.
- [47] Song Mei, Andrea Montanari, and Phan-Minh Nguyen. A Mean Field View of the Landscape of Two-Layers Neural Networks. *arXiv e-prints*, page arXiv:1804.06561, April 2018.
- [48] Ari S Morcos, Haonan Yu, Michela Paganini, and Yuandong Tian. One ticket to win them all: generalizing lottery ticket initializations across datasets and optimizers. *arXiv preprint arXiv:1906.02773*, 2019.
- [49] Preetum Nakkiran, Gal Kaplun, Yamini Bansal, Tristan Yang, Boaz Barak, and Ilya Sutskever. Deep Double Descent: Where Bigger Models and More Data Hurt. *arXiv e-prints*, page arXiv:1912.02292, December 2019.
- [50] George L Nemhauser, Laurence A Wolsey, and Marshall L Fisher. An analysis of approximations for maximizing submodular set functions—i. *Mathematical programming*, 14(1):265–294, 1978.
- [51] Arild Nøkland and Lars Hiller Eidnes. Training neural networks with local error signals. In *International Conference on Machine Learning*, pages 4839–4850. PMLR, 2019.
- [52] Laurent Orseau, Marcus Hutter, and Omar Rivasplata. Logarithmic Pruning is All You Need. *arXiv e-prints*, page arXiv:2006.12156, June 2020.
- [53] Samet Oymak and Mahdi Soltanolkotabi. Towards moderate overparameterization: global convergence guarantees for training shallow neural networks. *arXiv e-prints*, page arXiv:1902.04674, February 2019.
- [54] Tony Peng and Michael Sarazen. The staggering cost of training sota ai models, June 2019.
- [55] Ankit Pensia, Shashank Rajput, Alliot Nagle, Harit Vishwakarma, and Dimitris Papailiopoulos. Optimal lottery tickets via subsetsum: Logarithmic over-parameterization is sufficient. *arXiv preprint arXiv:2006.07990*, 2020.
- [56] Sebastian Pokutta, Christoph Spiegel, and Max Zimmer. Deep Neural Network Training with Frank-Wolfe. *arXiv e-prints*, page arXiv:2010.07243, October 2020.
- [57] Vivek Ramanujan, Mitchell Wortsman, Aniruddha Kembhavi, Ali Farhadi, and Mohammad Rastegari. What’s Hidden in a Randomly Weighted Neural Network? *arXiv e-prints*, page arXiv:1911.13299, November 2019.
- [58] Alex Renda, Jonathan Frankle, and Michael Carbin. Comparing Rewinding and Fine-tuning in Neural Network Pruning. *arXiv e-prints*, page arXiv:2003.02389, March 2020.
- [59] Mark Sandler, Andrew Howard, Menglong Zhu, Andrey Zhmoginov, and Liang-Chieh Chen. Mobilenetv2: Inverted residuals and linear bottlenecks. In *Proceedings of the IEEE conference on computer vision and pattern recognition*, pages 4510–4520, 2018.

- [60] Or Sharir, Barak Peleg, and Yoav Shoham. The cost of training nlp models: A concise overview. *arXiv preprint arXiv:2004.08900*, 2020.
- [61] Emma Strubell, Ananya Ganesh, and Andrew McCallum. Energy and policy considerations for deep learning in nlp. *arXiv preprint arXiv:1906.02243*, 2019.
- [62] Chaoqi Wang, Guodong Zhang, and Roger Grosse. Picking winning tickets before training by preserving gradient flow. *arXiv preprint arXiv:2002.07376*, 2020.
- [63] Chaoqi Wang, Guodong Zhang, and Roger Grosse. Picking Winning Tickets Before Training by Preserving Gradient Flow. *arXiv e-prints*, page arXiv:2002.07376, February 2020.
- [64] Ruibin Xiong, Yunchang Yang, Di He, Kai Zheng, Shuxin Zheng, Chen Xing, Huishuai Zhang, Yanyan Lan, Liwei Wang, and Tie-Yan Liu. On Layer Normalization in the Transformer Architecture. *arXiv e-prints*, page arXiv:2002.04745, February 2020.
- [65] Mao Ye, Chengyue Gong, Lizhen Nie, Denny Zhou, Adam Klivans, and Qiang Liu. Good subnetworks provably exist: Pruning via greedy forward selection. In *International Conference on Machine Learning*, pages 10820–10830. PMLR, 2020.
- [66] Mao Ye, Lemeng Wu, and Qiang Liu. Greedy Optimization Provably Wins the Lottery: Logarithmic Number of Winning Tickets is Enough. *arXiv e-prints*, page arXiv:2010.15969, October 2020.
- [67] Haoran You, Chaojian Li, Pengfei Xu, Yonggan Fu, Yue Wang, Xiaohan Chen, Richard G Baraniuk, Zhangyang Wang, and Yingyan Lin. Drawing early-bird tickets: Towards more efficient training of deep networks. *arXiv preprint arXiv:1909.11957*, 2019.
- [68] Ruichi Yu, Ang Li, Chun-Fu Chen, Jui-Hsin Lai, Vlad I. Morariu, Xintong Han, Mingfei Gao, Ching-Yung Lin, and Larry S. Davis. NISP: Pruning Networks using Neuron Importance Score Propagation. *arXiv e-prints*, page arXiv:1711.05908, November 2017.
- [69] Xiao Zhang, Yaodong Yu, Lingxiao Wang, and Quanquan Gu. Learning one-hidden-layer relu networks via gradient descent. In *The 22nd International Conference on Artificial Intelligence and Statistics*, pages 1524–1534. PMLR, 2019.
- [70] Hattie Zhou, Janice Lan, Rosanne Liu, and Jason Yosinski. Deconstructing Lottery Tickets: Zeros, Signs, and the Supermask. *arXiv e-prints*, page arXiv:1905.01067, May 2019.
- [71] Michael Zhu and Suyog Gupta. To prune, or not to prune: exploring the efficacy of pruning for model compression. *arXiv e-prints*, page arXiv:1710.01878, October 2017.
- [72] Zhuangwei Zhuang, Mingkui Tan, Bohan Zhuang, Jing Liu, Yong Guo, Qingyao Wu, Junzhou Huang, and Jinhui Zhu. Discrimination-aware Channel Pruning for Deep Neural Networks. *arXiv e-prints*, page arXiv:1810.11809, October 2018.

A Proofs

A.1 Convergence Analysis

Prior to presenting the proofs of the main theoretical results, we introduce several relevant technical lemmas.

Lemma 1. Consider $\mathbf{u}_k, \mathbf{u}_{k-1} \in \mathcal{M}_N$, representing adjacent iterates of (8)-(10) at step k . Additionally, consider an arbitrary update $\mathbf{q} \in \text{Vert}(\mathcal{M}_N)$, such that $\mathbf{z}_k = \mathbf{z}_{k-1} + \mathbf{q}$ and $\mathbf{u}_k = \frac{1}{k}\mathbf{z}_k$. Then, we can derive the following expression for the difference between adjacent iterates of (??):

$$\mathbf{u}_k - \mathbf{u}_{k-1} = \frac{1}{k}(\mathbf{q} - \mathbf{u}_{k-1})$$

Lemma 2. Because the objective $\ell(\cdot)$, defined over the space \mathcal{M}_N , is both quadratic and convex, the following expressions hold for any $\mathbf{s} \in \mathcal{M}_N$:

$$\begin{aligned} \ell(\mathbf{s}) &\geq \ell(\mathbf{u}_{k-1}) + \langle \nabla \ell(\mathbf{u}_{k-1}), \mathbf{s} - \mathbf{u}_{k-1} \rangle \\ \ell(\mathbf{s}) &\leq \ell(\mathbf{u}_{k-1}) + \langle \nabla \ell(\mathbf{u}_{k-1}), \mathbf{s} - \mathbf{u}_{k-1} \rangle + \|\mathbf{s} - \mathbf{u}_{k-1}\|_2^2 \end{aligned}$$

Observation 1. From Lemma 2, we can derive the following inequality.

$$\begin{aligned} \mathcal{L}_N &\geq \mathcal{L}_N^* = \min_{\mathbf{s} \in \mathcal{M}_N} \ell(\mathbf{s}) \\ &\geq \min_{\mathbf{s} \in \mathcal{M}_N} \{ \ell(\mathbf{u}_{k-1}) + \langle \nabla \ell(\mathbf{u}_{k-1}), \mathbf{s} - \mathbf{u}_{k-1} \rangle \} \\ &= \ell(\mathbf{u}_{k-1}) + \langle \nabla \ell(\mathbf{u}_{k-1}), \mathbf{s}_k - \mathbf{u}_{k-1} \rangle. \end{aligned}$$

Lemma 3. Assume there exists a sequence of values $\{z_k\}_{k \geq 0}$ such that $z_0 = 0$ and

$$|z_{k+1}|^2 \leq |z_k|^2 - 2\beta|z_k| + C, \quad \forall k \geq 0$$

where C and β are positive constants. Then, it must be the case that $|z_k| \leq \max\left(\sqrt{C}, \frac{C}{2}, \frac{C}{2\beta}\right)$ for $k > 0$.

Proof. We use an inductive argument to prove the above claim. For the base case of $z_0 = 0$, the claim is trivially true because $|z_0| = 0 \leq \max\left(\sqrt{C}, \frac{C}{2}, \frac{C}{2\beta}\right)$. For the inductive case, we define $f(x) = x^2 - 2\beta x + C$. It should be noted that $f(\cdot)$ is a 1-dimensional convex function. Therefore, given some closed interval $[a, b]$ within the domain of f , the maximum value of f over this interval must be achieved on one of the end points. This fact simplifies to the following expression, where a and b are two values within the domain of f such that $a \leq b$.

$$\max_{x \in [a, b]} f(x) = \max\{f(a), f(b)\}$$

From here, we begin the inductive step, for which we consider two cases.

Case 1: Assume that $|z_k| \leq \frac{C}{2\beta}$. Then, the following expression for $|z_{k+1}|$ can be derived.

$$\begin{aligned} |z_{k+1}|^2 &\leq f(|z_k|) \leq \max_z \left\{ f(z) : z \in \left[0, \frac{C}{2\beta}\right] \right\} = \max \left\{ f(0), f\left(\frac{C}{2\beta}\right) \right\} \\ &= \max \left\{ C, \frac{C^2}{4\beta^2} \right\} \leq \left[\max \left(\sqrt{C}, \frac{C}{2}, \frac{C}{2\beta} \right) \right]^2 \end{aligned}$$

Case 2: Assume that $|z_k| \geq \frac{C}{2\beta}$. Then, the following expression can be derived.

$$|z_{k+1}|^2 \leq |z_k|^2 - 2\beta|z_k| + C \stackrel{i)}{\leq} |z_k|^2 \leq \left[\max \left(\sqrt{C}, \frac{C}{2}, \frac{C}{2\beta} \right) \right]^2$$

where $i)$ holds because $2\beta|z_k| \geq C$. In both cases, it is shown that $|z_{k+1}| \leq \max\left(\sqrt{C}, \frac{C}{2}, \frac{C}{2\beta}\right)$. Therefore, the lemma is shown to be true by induction. \square

A.1.1 Proof of Theorem 1

We now present the proof of Theorem 1.

Proof. We define $\mathcal{L}_N^* = \min_{\mathbf{s} \in \mathcal{M}_N} \ell(\mathbf{s})$. Additionally, we define \mathbf{s}_k as follows.

$$\mathbf{s}_k = \arg \min_{\mathbf{s} \in \mathcal{M}_N} \{\langle \nabla \ell(\mathbf{u}_{k-1}), \mathbf{s} - \mathbf{u}_{k-1} \rangle\} = \arg \min_{\mathbf{s} \in \text{Vert}(\mathcal{M}_N)} \{\langle \nabla \ell(\mathbf{u}_{k-1}), \mathbf{s} - \mathbf{u}_{k-1} \rangle\}.$$

The second equality holds because a linear objective is being optimized on a convex polytope \mathcal{M}_N . Thus, the solution to this optimization is known to be achieved on some vertex $\mathbf{v} \in \text{Vert}(\mathcal{M}_N)$. Recall, as stated in Section 2, that $\mathcal{D}_{\mathcal{M}_N}$ denotes the diameter of the marginal polytope \mathcal{M}_N .

We assume the existence of some global two-layer neural network with N hidden neurons from which the pruned network is derived. It should be noted that the N neurons of this global network are used to define the vertices $\mathbf{v} \in \text{Vert}(\mathcal{M}_N)$ as described in Section 2. As a result, the loss of this global network, which we denote as \mathcal{L}_N , is the loss achieved by a uniform average over the N vertices of \mathcal{M}_N (i.e., see (1)). In other words, the loss of the global network at the time of pruning is given by the expression below.

$$\mathcal{L}_N = \ell \left(\frac{1}{N} \sum_{\mathbf{v} \in \text{Vert}(\mathcal{M}_N)} \mathbf{v} \right)$$

It is trivially known that $\mathcal{L}_N \geq \mathcal{L}_N^*$. Intuitively, the value of \mathcal{L}_N has an implicit dependence on the amount of training underwent by the global network. However, we make no assumptions regarding the global network's training (i.e., \mathcal{L}_N can be arbitrarily large for the purposes of this analysis). Using Observation 1, as well as Lemmas 1 and 2, we derive the following expression for the loss of iterates obtained with (10).

$$\begin{aligned} \ell(\mathbf{u}_k) &\stackrel{i)}{=} \min_{\mathbf{q} \in \text{Vert}(\mathcal{M}_N)} \ell \left(\frac{1}{k} (\mathbf{z}_{k-1} + \mathbf{q}) \right) \\ &\stackrel{ii)}{\leq} \ell \left(\frac{1}{k} (\mathbf{z}_{k-1} + \mathbf{s}_k) \right) \\ &\stackrel{iii)}{\leq} \ell(\mathbf{u}_{k-1}) + \left\langle \nabla \ell(\mathbf{u}_{k-1}), \frac{1}{k} (\mathbf{z}_{k-1} + \mathbf{s}_k) - \mathbf{u}_{k-1} \right\rangle + \left\| \frac{1}{k} (\mathbf{z}_{k-1} + \mathbf{s}_k) - \mathbf{u}_{k-1} \right\|_2^2 \\ &\stackrel{iv)}{=} \ell(\mathbf{u}_{k-1}) + \left\langle \nabla \ell(\mathbf{u}_{k-1}), \frac{1}{k} (\mathbf{s}_k - \mathbf{u}_{k-1}) \right\rangle + \left\| \frac{1}{k} (\mathbf{s}_k - \mathbf{u}_{k-1}) \right\|_2^2 \\ &\stackrel{v)}{\leq} \ell(\mathbf{u}_{k-1}) + \left\langle \nabla \ell(\mathbf{u}_{k-1}), \frac{1}{k} (\mathbf{s}_k - \mathbf{u}_{k-1}) \right\rangle + \frac{1}{k^2} \cdot \mathcal{D}_{\mathcal{M}_N}^2 \\ &= \ell(\mathbf{u}_{k-1}) + \frac{1}{k} \langle \nabla \ell(\mathbf{u}_{k-1}), \mathbf{s}_k - \mathbf{u}_{k-1} \rangle + \frac{1}{k^2} \cdot \mathcal{D}_{\mathcal{M}_N}^2 \\ &\stackrel{vi)}{\leq} \left(1 - \frac{1}{k} \right) \ell(\mathbf{u}_{k-1}) + \frac{1}{k} \cdot \mathcal{L}_N^* + \frac{1}{k^2} \cdot \mathcal{D}_{\mathcal{M}_N}^2 \\ &\stackrel{vii)}{\leq} \left(1 - \frac{1}{k} \right) \ell(\mathbf{u}_{k-1}) + \frac{1}{k} \cdot \mathcal{L}_N + \frac{1}{k^2} \cdot \mathcal{D}_{\mathcal{M}_N}^2 \end{aligned}$$

where *i)* is due to (8)-(10), *ii)* is because $\mathbf{s}_k \in \text{Vert}(\mathcal{M}_N)$, *iii)* is from Lemma 2, *iv)* is from Lemma 1 since it holds $\frac{1}{k} \mathbf{z}_{k-1} - \mathbf{u}_{k-1} = -\frac{1}{k} \mathbf{u}_{k-1} \Rightarrow \mathbf{u}_{k-1} = \frac{1}{k-1} \mathbf{z}_{k-1}$, *v)* is from the definition of $\mathcal{D}_{\mathcal{M}_N}$, and *vi) - vii)* are due to Observation 1. This expression can then be rearranged to yield the following recursive expression:

$$\begin{aligned} \ell(\mathbf{u}_k) &\leq \left(1 - \frac{1}{k} \right) \ell(\mathbf{u}_{k-1}) + \frac{1}{k} \cdot \mathcal{L}_N + \frac{1}{k^2} \cdot \mathcal{D}_{\mathcal{M}_N}^2 \Rightarrow \\ \ell(\mathbf{u}_k) - \mathcal{L}_N - \frac{1}{k} \cdot \mathcal{D}_{\mathcal{M}_N}^2 &\leq \left(1 - \frac{1}{k} \right) \cdot \left(\ell(\mathbf{u}_{k-1}) - \mathcal{L}_N - \frac{1}{k} \cdot \mathcal{D}_{\mathcal{M}_N}^2 \right) \end{aligned}$$

By unrolling the recursion in this expression over k iterations, we get the following:

$$\begin{aligned} \ell(\mathbf{u}_k) - \mathcal{L}_N - \frac{1}{k} \cdot \mathcal{D}_{\mathcal{M}_N}^2 &\leq \prod_{i=2}^k \left(1 - \frac{1}{i}\right) \cdot \left(\ell(\mathbf{u}_1) - \mathcal{L}_N - \frac{1}{2} \cdot \mathcal{D}_{\mathcal{M}_N}^2\right) \Rightarrow \\ \ell(\mathbf{u}_k) - \mathcal{L}_N - \frac{1}{k} \cdot \mathcal{D}_{\mathcal{M}_N}^2 &\leq \frac{1}{k} \cdot \left(\ell(\mathbf{u}_1) - \mathcal{L}_N - \frac{1}{2} \cdot \mathcal{D}_{\mathcal{M}_N}^2\right) \end{aligned}$$

By rearranging terms, we arrive at the desired expression

$$\ell(\mathbf{u}_k) \leq \frac{1}{k} \cdot \left(\ell(\mathbf{u}_1) - \mathcal{L}_N + \frac{1}{2} \cdot \mathcal{D}_{\mathcal{M}_N}^2\right) + \mathcal{L}_N \leq \mathcal{O}\left(\frac{1}{k}\right) + \mathcal{L}_N \quad (13)$$

□

A.1.2 Proof of Theorem 3

Now, we provide the proof for the faster convergence rate stated in Theorem 3.

Proof. We define $\mathbf{w}_k = k(\mathbf{y} - \mathbf{u}_k)$. Also recall that $\ell(\mathbf{z}) = \frac{1}{2} \|\mathbf{z} - \mathbf{y}\|_2^2$. Furthermore, we define \mathbf{s}_{k+1} as follows.

$$\begin{aligned} \mathbf{s}_{k+1} &= \arg \min_{\mathbf{s} \in \mathcal{M}_N} \nabla \ell(\mathbf{u}_k)^\top (\mathbf{s} - \mathbf{u}_k) \\ &= \arg \min_{\mathbf{s} \in \mathcal{M}_N} \langle \nabla \ell(\mathbf{u}_k), \mathbf{s} - \mathbf{u}_k \rangle \\ &\stackrel{i)}{=} \arg \min_{\mathbf{s} \in \mathcal{M}_N} \langle \mathbf{u}_k - \mathbf{y}, \mathbf{s} - \mathbf{u}_k \rangle \\ &= \arg \min_{\mathbf{s} \in \mathcal{M}_N} \langle -\mathbf{w}_k, \mathbf{s} - \mathbf{u}_k \rangle \\ &= \arg \min_{\mathbf{s} \in \mathcal{M}_N} \langle \mathbf{w}_k, \mathbf{u}_k - \mathbf{s} \rangle \\ &= \arg \min_{\mathbf{s} \in \mathcal{M}_N} \{ \langle \mathbf{w}_k, \mathbf{u}_k \rangle + \langle \mathbf{w}_k, -\mathbf{s} \rangle \} \\ &= \arg \min_{\mathbf{s} \in \mathcal{M}_N} \langle \mathbf{w}_k, -\mathbf{s} \rangle \\ &= \arg \min_{\mathbf{s} \in \mathcal{M}_N} \langle \mathbf{w}_k, \mathbf{y} - \mathbf{s} \rangle \end{aligned}$$

where $i)$ follows from (5). Notice that \mathbf{s}_k minimizes a linear objective (i.e., the dot product with \mathbf{w}_k) over the domain of the marginal polytope \mathcal{M}_N . As a result, the optimum is achieved on a vertex of the marginal polytope, implying that $\mathbf{s}_k \in \text{Vert}(\mathcal{M}_N)$ for all $k > 0$. We assume that $\mathcal{B}(\mathbf{y}, \gamma) \in \mathcal{M}_N$. Under this assumption, it is known that $\mathbf{s}^* = \mathbf{y} + \gamma \frac{\mathbf{w}_k}{\|\mathbf{w}_k\|_2} \in \mathcal{M}_N$, which allows the following to be derived.

$$\begin{aligned} \langle \mathbf{w}_k, \mathbf{y} - \mathbf{s}_{k+1} \rangle &= \min_{\mathbf{s} \in \mathcal{M}_N} \langle \mathbf{w}_k, \mathbf{y} - \mathbf{s} \rangle \\ &\leq \langle \mathbf{w}_k, \mathbf{y} - \mathbf{s}^* \rangle \\ &= -\gamma \|\mathbf{w}_k\|_2 \end{aligned} \quad (14)$$

From (10), the following expressions for \mathbf{u}_k and \mathbf{q}_k can be derived.

$$\mathbf{u}_k = \frac{1}{k} \cdot \mathbf{z}_k = \frac{1}{k} \cdot [(k-1)\mathbf{u}_{k-1} + \mathbf{q}_k] \quad (15)$$

$$\begin{aligned} \mathbf{q}_k &= \arg \min_{\mathbf{q} \in \text{Vert}(\mathcal{M}_N)} \ell\left(\frac{1}{k}[\mathbf{z}_{k-1} + \mathbf{q}]\right) \\ &= \arg \min_{\mathbf{q} \in \text{Vert}(\mathcal{M}_N)} \left\| \frac{1}{k}[(k-1)\mathbf{u}_{k-1} + \mathbf{q}] - \mathbf{y} \right\|_2^2 \end{aligned} \quad (16)$$

Combining all of this together, the following expression can be derived for $\|\mathbf{w}_k\|_2^2$, where $\mathcal{D}_{\mathcal{M}_N}$ is the diameter of \mathcal{M}_N :

$$\begin{aligned}
\|\mathbf{w}_k\|_2^2 &= \|k(\mathbf{y} - \mathbf{u}_k)\|_2^2 = \|k(\mathbf{u}_k - \mathbf{y})\|_2^2 \\
&\stackrel{i)}{=} \min_{\mathbf{q} \in \mathcal{M}_N} \|k(\frac{1}{k}[(k-1)\mathbf{u}_{k-1} + \mathbf{q}] - \mathbf{y})\|_2^2 \\
&= \min_{\mathbf{q} \in \mathcal{M}_N} \|(k-1)\mathbf{u}_{k-1} + \mathbf{q} - k\mathbf{y}\|_2^2 \\
&= \min_{\mathbf{q} \in \mathcal{M}_N} \|-(k-1)\mathbf{y} + (k-1)\mathbf{u}_{k-1} + \mathbf{q} - \mathbf{y}\|_2^2 \\
&= \min_{\mathbf{q} \in \mathcal{M}_N} \|-\mathbf{w}_{k-1} - \mathbf{y} + \mathbf{q}\|_2^2 \\
&= \min_{\mathbf{q} \in \mathcal{M}_N} \|\mathbf{w}_{k-1} + \mathbf{y} - \mathbf{q}\|_2^2 \\
&\stackrel{ii)}{\leq} \|\mathbf{w}_{k-1} + \mathbf{y} - \mathbf{s}_k\|_2^2 \\
&= \|\mathbf{w}_{k-1}\|_2^2 + 2\langle \mathbf{w}_{k-1}, \mathbf{y} - \mathbf{s}_k \rangle + \|\mathbf{y} - \mathbf{s}_k\|_2^2 \\
&\leq \|\mathbf{w}_{k-1}\|_2^2 + 2\langle \mathbf{w}_{k-1}, \mathbf{y} - \mathbf{s}_k \rangle + \mathcal{D}_{\mathcal{M}_N}^2 \\
&\stackrel{iii)}{\leq} \|\mathbf{w}_{k-1}\|_2^2 - 2\gamma\|\mathbf{w}_{k-1}\|_2 + \mathcal{D}_{\mathcal{M}_N}^2
\end{aligned}$$

where *i*) follows from (15) and (16), *ii*) follows from the fact that $\mathbf{s}_k \in \mathcal{M}_N$, and *iii*) follows from (14). Therefore, from this analysis, the following recursive expression for the value of $\|\mathbf{w}_k\|_2^2$ is derived:

$$\|\mathbf{w}_k\|_2^2 \leq \|\mathbf{w}_{k-1}\|_2^2 - 2\gamma\|\mathbf{w}_{k-1}\|_2 + \mathcal{D}_{\mathcal{M}_N}^2 \quad (17)$$

Then, by invoking Lemma 3, we derive the following inequality.

$$\begin{aligned}
\|\mathbf{w}_k\|_2^2 &\leq \max \left\{ \mathcal{D}_{\mathcal{M}_N}, \frac{\mathcal{D}_{\mathcal{M}_N}^2}{2}, \frac{\mathcal{D}_{\mathcal{M}_N}^2}{2\gamma} \right\} \\
&= \mathcal{O} \left(\frac{1}{\min(1, \gamma)} \right)
\end{aligned}$$

With this in mind, the following expression can then be derived for the loss $\ell(\mathbf{u}_k)$ achieved by (8)-(10) after k iterations.

$$\ell(\mathbf{u}_k) = \frac{1}{2}\|\mathbf{u}_k - \mathbf{y}\|_2^2 = \frac{\|\mathbf{w}_k\|_2^2}{2k^2} = \mathcal{O} \left(\frac{1}{k^2 \min(1, \gamma)^2} \right)$$

This yields the desired expression, thus completing the proof. \square

A.2 Training Analysis

Prior to analyzing the amount of training needed for a good pruning loss, several supplemental theorems and lemmas exist that must be introduced. From [53], we utilize theorems regarding the convergence rates of two-layer neural networks trained with GD and SGD. We begin with the theorem for the convergence of GD in Theorem 4, then provide the associated convergence rate for SGD within Theorem 5. Both Theorems 4 and 5 are simply restated from [53] for convenience purposes.

Theorem 4 ([53]). *Assume there exists a two-layer neural network and associated dataset as described in Section 2. Denote N as the number of hidden neurons in the two-layer neural network, m as the number of unique examples in the dataset, and d as the input dimension of examples in the dataset. Assume without loss of generality that the input data within the dataset is normalized so that $\|\mathbf{x}^{(i)}\|_2 = 1$ for all $i \in [m]$. A moderate amount of overparameterization within the two-layer network is assumed, given by $Nd > m^2$. Furthermore, it is assumed that $m > d$ and that the first and second derivatives of the network's activation function are bounded (i.e., $|\sigma'_+(\cdot)| \leq \delta$ and $|\sigma''_+(\cdot)| \leq \delta$ for some $\delta \in \mathbb{R}$). Given these assumptions, the following bound is achieved with a high probability by training the neural network with gradient descent.*

$$\|f(\mathbf{X}, \Theta_t) - \mathbf{Y}\|_2 \leq \left(1 - c \frac{d}{m}\right)^t \cdot \|f(\mathbf{X}, \Theta_0) - \mathbf{Y}\|_2 \quad (18)$$

In (18), $c \in \mathbb{R}$, $\Theta_t = \{\theta_{1,t}, \dots, \theta_{N,t}\}$ represents the network weights at iteration t of gradient descent, $f(\cdot, \cdot) \in \mathbb{R}^m$ represents the network output over the full dataset $\mathbf{X} \in \mathbb{R}^{m \times d}$, and $\mathbf{Y} = [y^{(1)}, \dots, y^{(m)}]^T$ represents a vector of all dataset labels. Θ_0 is assumed to be randomly sampled from a normal distribution (i.e., $\Theta_0 \sim \mathcal{N}(0, 1)$).

Theorem 5 ([53]). *Here, all assumptions of Theorem 4 are adopted, but we assume the two-layer neural network is trained with SGD instead of GD. For SGD, parameter updates are performed over a sequence of randomly-sampled examples within the training dataset (i.e., the true gradient is not computed for each update). Given the assumptions, there exists some event E with probability $P[E] \geq \max\left(\kappa, 1 - c_1 \left(c_2 \sqrt{\frac{m}{d}}\right)^{\frac{1}{N^d}}\right)$, where $c_1, c_2, \kappa \in \mathbb{R}$, $0 \leq c_1 \leq \frac{4}{3}$, and $0 < \kappa \leq 1$. Given the event E , with high probability the following bound is achieved for training a two-layer neural network with SGD.*

$$\mathbb{E} [\|f(\mathbf{X}, \Theta_t) - \mathbf{Y}\|_2^2 \mathbb{1}_E] \leq \left(1 - c \frac{d}{m^2}\right)^t \cdot \|f(\mathbf{X}, \Theta_0) - \mathbf{Y}\|_2^2 \quad (19)$$

In (19), $c \in \mathbb{R}$, Θ_t represent the network weights at iteration t of SGD, $\mathbb{1}_E$ is the indicator function for event E , $f(\cdot, \cdot)$ represents the output of the two layer neural network over the entire dataset $\mathbf{X} \in \mathbb{R}^{m \times d}$, and $\mathbf{Y} \in \mathbb{R}^m$ represents a vector of all labels in the dataset.

It should be noted that the overparameterization assumptions within Theorems 4 and 5 are very mild, which leads us to adopt this analysis within our work. Namely, we only require that the number of examples in the dataset exceeds the input dimension and the number of parameters within the first neural network layer exceeds the squared size of the dataset. In comparison, previous work lower bounds the number of hidden neurons in the two-layer neural network (i.e., more restrictive than the number of parameters in the first layer) with higher-order polynomials of m to achieve similar convergence guarantees [1, 15, 38].

In comparing the convergence rates of Theorems 4 and 5, one can notice that these linear convergence rates are very similar. The extra factor of m within the denominator of Theorem 5 is intuitively due to the fact that m updates are performed in a single pass through the dataset for SGD, while GD uses the full dataset at every parameter update. Such alignment between the convergence guarantees for GD and SGD allows our analysis to be similar for both algorithms.

We now state a relevant technical lemma based on Theorem 1. Beginning from (13), the following can be shown.

Lemma 4. *Assume \mathbf{u}_k is the k -th iterate of (10). Then, the following is true.*

$$\ell(\mathbf{u}_k) \leq \frac{1}{k} \ell(\mathbf{u}_1) + \frac{1}{2k} \mathcal{D}_{\mathcal{M}_N}^2 + \frac{(k-1)}{k} \cdot \mathcal{L}_N$$

where \mathcal{L}_N is the loss achieved by a two-layer neural network of width N .

Proof. Recall, that $\mathcal{D}_{\mathcal{M}_N}$ represents the diameter of the marginal polytope \mathcal{M}_N . Beginning with (13), the following can be shown.

$$\begin{aligned} \ell(\mathbf{u}_k) &\leq \frac{1}{k} \left(\ell(\mathbf{u}_1) - \mathcal{L}_N + \frac{1}{2} \mathcal{D}_{\mathcal{M}_N}^2 \right) + \mathcal{L}_N \\ &= \frac{1}{k} \left(\ell(\mathbf{u}_1) + \frac{1}{2} \mathcal{D}_{\mathcal{M}_N}^2 \right) + \frac{k-1}{k} \mathcal{L}_N \\ &= \frac{1}{k} \ell(\mathbf{u}_1) + \frac{1}{2k} \mathcal{D}_{\mathcal{M}_N}^2 + \frac{k-1}{k} \mathcal{L}_N \end{aligned}$$

□

Observation 2. *We commonly refer to the value of \mathcal{L}_N , representing the quadratic loss of the two-layer network over the full dataset. The value of \mathcal{L}_N can be expressed as follows.*

$$\mathcal{L}_N = \ell \left(\frac{1}{N} \sum_{\mathbf{v} \in \text{Vert}(\mathcal{M}_N)} \mathbf{v} \right) = \frac{1}{2m} \|f(\mathbf{X}, \Theta) - \mathbf{Y}\|_2^2$$

The expression above is derived by simply applying the definitions associated with $\ell(\cdot)$ that are provided in Section 2.

A.2.1 Proof of Theorem 2

We now provide the proof for Theorem 2.

Proof. From Theorem 5, we have a bound for $\mathbb{E} [\|f(\mathbf{X}, \Theta_t) - \mathbf{Y}\|_2^2 \mathbb{1}_E]$, where $\|f(\mathbf{X}, \Theta_t) - \mathbf{Y}\|_2^2$ represents the loss over the entire dataset after t iterations of SGD (i.e., without the factor of $\frac{1}{2}$). Two sources of stochasticity exist within the expectation expression $\mathbb{E} [\|f(\mathbf{X}, \Theta_t) - \mathbf{Y}\|_2^2 \mathbb{1}_E]$: *i*) randomness over the event E and *ii*) randomness over the t -th iteration of SGD given the first $t - 1$ iterations. The probability of event E is independent of the randomness over SGD iterations, which allows the following expression to be derived.

$$\begin{aligned} \mathbb{E} [\|f(\mathbf{X}, \Theta_t) - \mathbf{Y}\|_2^2 \mathbb{1}_E] &\stackrel{i)}{=} \mathbb{E} [\|f(\mathbf{X}, \Theta_t) - \mathbf{Y}\|_2^2] \cdot \mathbb{E} [\mathbb{1}_E] \\ &\stackrel{ii)}{\geq} \max \left(\kappa, 1 - c_1 \left(c_2 \sqrt{\frac{m}{d}} \right)^{\frac{1}{Nd}} \right) \mathbb{E} [\|f(\mathbf{X}, \Theta_t) - \mathbf{Y}\|_2^2] \end{aligned}$$

where *i*) holds from the independence of expectations and *ii*) is derived from the probability expression for event E in Theorem 5. Combining the above expression with (19) from Theorem 5 yields the following, where two possible cases exist.

Case 1: $\max \left(\kappa, 1 - c_1 \left(c_2 \sqrt{\frac{m}{d}} \right)^{\frac{1}{Nd}} \right) = 1 - c_1 \left(c_2 \sqrt{\frac{m}{d}} \right)^{\frac{1}{Nd}}$

$$\begin{aligned} \left(1 - c_1 \left(c_2 \sqrt{\frac{m}{d}} \right)^{\frac{1}{Nd}} \right) \mathbb{E} [\|f(\mathbf{X}, \Theta_t) - \mathbf{Y}\|_2^2] &\leq \left(1 - c \frac{d}{m^2} \right)^t \|f(\mathbf{X}, \Theta_0) - \mathbf{Y}\|_2^2 \Rightarrow \\ \mathbb{E} [\|f(\mathbf{X}, \Theta_t) - \mathbf{Y}\|_2^2] &\leq \left(1 - c_1 \left(c_2 \sqrt{\frac{m}{d}} \right)^{\frac{1}{Nd}} \right)^{-1} \left(1 - c \frac{d}{m^2} \right)^t \|f(\mathbf{X}, \Theta_0) - \mathbf{Y}\|_2^2 \quad (20) \end{aligned}$$

Case 2: $\max \left(\kappa, 1 - c_1 \left(c_2 \sqrt{\frac{m}{d}} \right)^{\frac{1}{Nd}} \right) = \kappa$

$$\begin{aligned} \kappa \cdot \mathbb{E} [\|f(\mathbf{X}, \Theta_t) - \mathbf{Y}\|_2^2] &\leq \left(1 - c \frac{d}{m^2} \right)^t \|f(\mathbf{X}, \Theta_0) - \mathbf{Y}\|_2^2 \Rightarrow \\ \mathbb{E} [\|f(\mathbf{X}, \Theta_t) - \mathbf{Y}\|_2^2] &\leq \kappa^{-1} \left(1 - c \frac{d}{m^2} \right)^t \|f(\mathbf{X}, \Theta_0) - \mathbf{Y}\|_2^2 \quad (21) \end{aligned}$$

From Observation 2, we can derive the following, where the expectation is with respect to randomness over SGD iterations (i.e., we assume the global two-layer network of width N is trained with SGD).

$$\begin{aligned} \mathbb{E}[\mathcal{L}_N] &= \mathbb{E} \left[\frac{1}{2m} \|f(\mathbf{X}, \Theta_t) - \mathbf{Y}\|_2^2 \right] \\ &\stackrel{i)}{=} \frac{1}{2m} \mathbb{E} [\|f(\mathbf{X}, \Theta_t) - \mathbf{Y}\|_2^2] \end{aligned}$$

Here, the equality in *i*) holds true because $\frac{1}{2m}$ is a constant value given a fixed dataset. Then, the above expression can be combined with (20) and (21) to yield the following.

$$\mathbb{E}[\mathcal{L}_N] \leq \frac{1}{2m} \left[\max \left(\kappa, \left(1 - c_1 \left(c_2 \sqrt{\frac{m}{d}} \right)^{\frac{1}{Nd}} \right) \right) \right]^{-1} \left(1 - c \frac{d}{m^2} \right)^t \|f(\mathbf{X}, \Theta_0) - \mathbf{Y}\|_2^2 \quad (22)$$

Then, we can substitute (22) into Lemma 4 as follows, where expectations are with respect to randomness over SGD iterations. We also define $\mathcal{L}_0 = \|f(\mathbf{X}, \Theta_0) - \mathbf{Y}\|_2^2$ and $\zeta =$

$$\begin{aligned}
& \left[\max \left(\kappa, \left(1 - c_1 \left(c_2 \sqrt{\frac{m}{d}} \right)^{\frac{1}{Nd}} \right) \right) \right]^{-1}. \\
\mathbb{E}[\ell(\mathbf{u}_k)] & \leq \frac{1}{k} \mathbb{E}[\ell(\mathbf{u}_1)] + \frac{1}{2k} \mathbb{E}[\mathcal{D}_{\mathcal{M}_N}^2] + \frac{k-1}{k} \mathbb{E}[\mathcal{L}_N] \\
& \leq \frac{1}{k} \mathbb{E}[\ell(\mathbf{u}_1)] + \frac{1}{2k} \mathbb{E}[\mathcal{D}_{\mathcal{M}_N}^2] + \frac{(k-1)\zeta}{2mk} \left(1 - c \frac{d}{m^2} \right)^t \|f(\mathbf{X}, \Theta_0) - \mathbf{Y}\|_2^2 \\
& = \frac{1}{k} \mathbb{E}[\ell(\mathbf{u}_1)] + \frac{1}{2k} \mathbb{E}[\mathcal{D}_{\mathcal{M}_N}^2] + \frac{(k-1)\zeta}{2mk} \left(1 - c \frac{d}{m^2} \right)^t \mathcal{L}_0 \tag{23}
\end{aligned}$$

In (23), it can be seen that all terms on the right-hand-side of the equation will decay to zero as k increases aside from the rightmost term. The rightmost term of (23) will remain relatively fixed as k increases due to its factor of $k-1$ in the numerator. Within (23), there are two parameters that can be modified by the practitioner: N and t (i.e., notice that ζ depends on N). All other factors within the expressions are constants based on the dataset that cannot be modified. N only appears in the $1 - c_1 \left(c_2 \sqrt{\frac{m}{d}} \right)^{\frac{1}{Nd}}$ factor of ζ , thus revealing that the value of N cannot be naively increased within (23) to remove the factor of $k-1$.

To determine how t can be modified to achieve a better pruning rate, we notice that a setting of $\left(1 - c \frac{d}{m^2} \right)^t = \mathcal{O}\left(\frac{1}{k}\right)$ would cancel the factor of $k-1$ in (23). With this in mind, we observe the following.

$$\begin{aligned}
\left(1 - c \frac{d}{m^2} \right)^t & = \mathcal{O}\left(\frac{1}{k}\right) \Rightarrow \\
t \cdot \log\left(1 - c \frac{d}{m^2} \right) & = \mathcal{O}(-\log(k)) \Rightarrow \\
t & = \frac{\mathcal{O}(-\log(k))}{\log\left(1 - c \frac{d}{m^2} \right)} \Rightarrow \\
t & \approx \mathcal{O}\left(\frac{-\log(k)}{\log\left(1 - c \frac{d}{m^2} \right)} \right) \tag{24}
\end{aligned}$$

If the amount of training in (24) is satisfied, the factor of $k-1$ in the rightmost term in Eq. (23) will be canceled, causing the expected pruning loss to decay as k increases. Based on Theorem 5, it must be the case that $\left(1 - c \frac{d}{m^2} \right) \in [0, 1]$ in order for SGD to converge. As a result, $\lim_{t \rightarrow \infty} \left(1 - c \frac{d}{m^2} \right)^t = 0$, causing the rightmost term in (23) to approach zero as $t \rightarrow \infty$. In other words, the value of t can increase beyond the bound in (24) without damaging the loss of the pruned network, as the rightmost term in (23) will simply become zero. This observation that t can increase beyond the value in (24) yields the final expression for the number of SGD iterations required to achieve the desired $\mathcal{O}\left(\frac{1}{k}\right)$ pruning rate.

$$t \gtrsim \mathcal{O}\left(\frac{-\log(k)}{\log\left(1 - c \frac{d}{m^2} \right)} \right)$$

□

A.2.2 Supplemental Result and Proof with GD

In addition to the proof of Theorem 2, we provide a similar result for neural networks trained with GD to further support our analysis of the amount of training required to achieve good loss via pruning.

Theorem 6. *Assume a two-layer neural network of width N was trained for t iterations with gradient descent over a dataset of size m . Furthermore, assume that $Nd > m^2$ and $m > d$, where d represents the input dimension of data in D . When the network is pruned via (8)-(10), it will achieve a loss*

$\mathcal{L}' \propto O(\frac{1}{k})$ if the number of gradient descent iterations t satisfies the following condition.

$$t \gtrsim O\left(\frac{-\log(k)}{\log(1 - c\frac{d}{m})}\right) \quad (25)$$

Otherwise, the loss of the pruned network will not improve during successive iterations of (8)-(10).

Proof. Beginning with Lemma 4, we can use Theorem 4 to arrive at the following expression. Here, we define $\mathcal{L}_0 = \|f(\mathbf{X}, \Theta_0) - \mathbf{Y}\|_2^2$ and define \mathcal{L}_N as described in Observation 2.

$$\begin{aligned} l(\mathbf{u}_k) &\leq \frac{1}{k}\ell(\mathbf{u}_1) + \frac{1}{2k}\mathcal{D}_{\mathcal{M}_N}^2 + \frac{k-1}{k}\mathcal{L}_N \\ &\stackrel{i)}{=} \frac{1}{k}\ell(\mathbf{u}_1) + \frac{1}{2k}\mathcal{D}_{\mathcal{M}_N}^2 + \frac{k-1}{2mk}\|f(\mathbf{X}, \Theta_t) - \mathbf{Y}\|_2^2 \\ &\stackrel{ii)}{\leq} \frac{1}{k}\ell(\mathbf{u}_1) + \frac{1}{2k}\mathcal{D}_{\mathcal{M}_N}^2 + \frac{k-1}{2k}\left(1 - c\frac{d}{m}\right)^{2t} \cdot \mathcal{L}_0 \end{aligned} \quad (26)$$

where *i)* is due to Observation 2 and *ii)* is from Theorem 4. From this expression, one can realize that an $O(\frac{1}{k})$ rate is only achieved if the factor of $k-1$ within the rightmost term of (26) is removed. This factor, if not counteracted, will cause the upper bound for $\ell(\mathbf{u}_k)$ to remain constant, as the right hand expression of (26) would be dominated by the value of \mathcal{L}_0 . However, this poor upper bound can be avoided by manipulating the $(1 - c\frac{d}{m})^{2t}$ term to eliminate the factor of $k-1$. For this to happen, it must be true that $(1 - c\frac{d}{m})^{2t} \approx O(\frac{1}{k})$, which allows the following asymptotic expression for t to be derived.

$$\begin{aligned} \left(1 - c\frac{d}{m}\right)^{2t} &= O\left(\frac{1}{k}\right) \Rightarrow \\ 2t \cdot \log\left(1 - c\frac{d}{m}\right) &= O(-\log(k)) \Rightarrow \\ t &= \frac{O(-\log(k))}{2 \cdot \log\left(1 - c\frac{d}{m}\right)} \Rightarrow \\ t &\approx O\left(\frac{-\log k}{\log\left(1 - c\frac{d}{m}\right)}\right) \end{aligned} \quad (27)$$

If the amount of training in (27) is satisfied, it allows the factor of $k-1$ in the rightmost term of 26 to be canceled. It is trivially true that $\lim_{t \rightarrow \infty} (1 - c\frac{d}{m})^{2t} = 0$ because $(1 - c\frac{d}{m}) \in [0, 1]$ if gradient descent converges; see Theorem 4. As a result, the rightmost term in (26) also approaches zero as t increases, allowing the $O(\frac{1}{k})$ pruning rate to be achieved. This observation that t can be increased beyond the value in (27) without issues leads to the final expression from Theorem 6.

$$t \gtrsim O\left(\frac{-\log(k)}{\log(1 - c\frac{d}{m})}\right)$$

□

B Empirical Analysis of $\mathbf{y} \in \mathcal{M}_N$

To achieve the faster rate provided in Theorem 3, we make the assumption that $B(\mathbf{y}, \gamma) \in \mathcal{M}_N$. If it is assumed that $\gamma > 0$, this assumption is slightly stronger than $\mathbf{y} \in \mathcal{M}_N$, as it implies \mathbf{y} cannot lie on the perimeter of \mathcal{M}_N . However, this assumption roughly requires that $\mathbf{y} \in \mathcal{M}_N$. Although previous work has attempted to analyze this assumption theoretically [65], it is not immediately clear whether this assumption is reasonable in practice.

We perform experiments using two-layer neural networks trained on different image classification datasets to determine if this assumption is satisfied in practice. Namely, we train a neural network

| m | MNIST-UNIFORM | | MNIST-TWO-CLASS | | CIFAR10-UNIFORM | | CIFAR10-TWO-CLASS | |
|------|---------------|-------------|-----------------|-------------|-----------------|-------------|-------------------|-------------|
| | LR | Num. Epochs | LR | Num. Epochs | LR | Num. Epochs | LR | Num. Epochs |
| 1000 | 1e-8 | 1 | 1e-8 | 1 | 1e-7 | 4 | 1e-8 | 1 |
| 2000 | 1e-8 | 1 | 1e-8 | 1 | 1e-8 | 7 | 1e-6 | 1 |
| 3000 | 1e-7 | 1 | 1e-8 | 1 | 1e-8 | 6 | 1e-7 | 1 |
| 4000 | 1e-7 | 1 | 1e-8 | 1 | 1e-7 | 9 | 1e-7 | 2 |
| 5000 | 1e-6 | 1 | 1e-8 | 1 | 1e-7 | 10 | 1e-7 | 1 |

Table 3: Results of empirically analyzing whether $\mathbf{y} \in \mathcal{M}_N$. For each of the possible datasets and sizes, we report the optimal learning rate and then number of training epochs required before the assumption was satisfied.

on downsampled versions of the MNIST and CIFAR10 datasets, as described in Section B.1. The two-layer network is randomly initialized and trained on each dataset and, following every epoch, the $\mathbf{y} \in \mathcal{M}_N$ condition is tested (i.e., see Section B.2 for details). We record the first epoch of training after which $\mathbf{y} \in \mathcal{M}_N$ is true and report the results in Table 3. As can be seen, *the assumption is satisfied for all datasets after minimal training in all cases*. In fact, the worst-case experiment only requires 10 epochs for $\mathbf{y} \in \mathcal{M}_N$ to be satisfied, revealing that the assumption is relatively mild in practice.

B.1 Models and Datasets

All tests were performed with a two-layer neural network as defined in Section 2. This model contains a single output neuron, N hidden neurons, and uses a smooth activation function (i.e., we use the sigmoid activation). For each test, we ensure the overparameterization requirements presented in Theorem 2 (i.e., $Nd > m^2$ and $m > d$, where N is the number of hidden neurons, d is the input dimension, and m is the size of the dataset) are satisfied. For simplicity, the network is trained without any data augmentation, batch normalization, or dropout.

Experiments are performed using the MNIST and CIFAR10 datasets. These datasets are reduced in size in order to make overparameterization assumptions within the two-layer neural network easier to satisfy. In particular, we perform tests with 1000, 2000, 3000, 4000, and 5000 dataset examples for each of the separate datasets. Because the two-layer neural network contains only a single output neuron, we modify the MNIST and CIFAR10 datasets into binary classification problems. The downsampling and binarization of datasets can be done in two possible ways, which are outlined below.

- **UNIFORM:** An even number of examples are randomly sampled from each class.⁷ Then, examples with a label greater than four are mapped to a label of one and vice versa.
- **TWO-CLASS:** We only consider examples from two unique classes in the dataset and randomly sample an even number of examples from each class.⁸ These two classes are mapped to a label of zero and one, respectively.

To further ease overparameterization requirements, CIFAR10 images are downsampled from a spatial resolution of 32×32 to a spatial resolution of 18×18 using bilinear interpolation. Dataset examples were flattened to produce a single input vector for each image, which can be passed as input to the two-layer neural network. The number of hidden neurons utilized for tests with different values of m are shown in Table 4, where the selected value of N is (roughly) the smallest round value to satisfy overparameterization assumptions. The hidden dimension of the two-layer network was kept constant between datasets because the CIFAR10 images were downsampled such that the input dimension is relatively similar to MNIST.

To improve training stability, we add a sigmoid activation function to the output neuron of the two-layer network and train the network with binary cross entropy loss. The addition of this output activation function slightly complicates the empirical determination of whether $\mathbf{y} \in \mathcal{M}_N$, which

⁷A uniformly-sampled dataset of size 1000 would contain 100 examples sampled from each of the ten classes.

⁸For MNIST we consider the classes six and nine, while for CIFAR10 we consider the airplane and automobile classes.

| m | N |
|----------|----------|
| 1000 | 1300 |
| 2000 | 6000 |
| 3000 | 12000 |
| 4000 | 21000 |
| 5000 | 32000 |

Table 4: Displays the hidden dimension of the two-layer neural network used to test the $\mathbf{y} \in \mathcal{M}_N$ assumption for different dataset sizes. Hidden dimensions are the same between tests with MNIST and CIFAR10.

is further described in Section B.2. Despite slightly deviating from the setup in Section 2, this modification greatly improves training stability and is more realistic (i.e., classification datasets are not regularly trained with ℓ_2 regression loss as described in Section 2). The network is trained using stochastic gradient descent.⁹ We adopt a batch size of one to match the stochastic gradient descent setting exactly and do not use any weight decay.

B.2 Determining Convex Hull Membership

As mentioned in Section 2, we define $\mathbf{y} = [y^{(1)}, y^{(2)}, \dots, y^{(m)}] / \sqrt{m}$ as a vector containing all labels in our dataset (i.e., in this case, a vector of binary labels). Furthermore, we define $\phi_{i,j} = \sigma(\mathbf{x}^{(j)}, \boldsymbol{\theta}_i)$ as the output of neuron i for example j in the dataset. These values can be concatenated as $\boldsymbol{\Phi}_i = [\phi_{i,1}, \phi_{i,2}, \dots, \phi_{i,m}] / \sqrt{m}$, forming a vector of output activations for each neuron over the entire dataset. Then, we define $\mathcal{M}_N = \text{Conv} \{ \boldsymbol{\Phi}_i : i \in [N] \}$. It should be noted that the activation vectors $\boldsymbol{\Phi}_i$ are obtained from the N neurons of a two-layer neural network that has been trained for any number of iterations T . For the experiments in this section, the vectors $\boldsymbol{\Phi}_i$ are computed after each epoch of training to determine whether $\mathbf{y} \in \mathcal{M}_N$, and we report the number for the first epoch in which this membership is satisfied.

The convex hull membership problem can be formulated as a linear program, and we utilize this formulation to empirically determine when $\mathbf{y} \in \mathcal{M}_N$. In particular, we consider the following linear program.

$$\begin{aligned}
& \min \mathbf{c}^\top \boldsymbol{\alpha} & (28) \\
& \text{such that } A\boldsymbol{\alpha} = \mathbf{y} \\
& Z\boldsymbol{\alpha} = \mathbf{1} \\
& \boldsymbol{\alpha} \geq \mathbf{0}
\end{aligned}$$

where $\mathbf{c} \in \mathbb{R}^N$ is an arbitrary cost vector, $A = (\boldsymbol{\Phi}_1 \dots \boldsymbol{\Phi}_N) \in \mathbb{R}^{m \times N}$, and $Z = (1 \dots 1) \in \mathbb{R}^{1 \times N}$, and $\boldsymbol{\alpha}$ is the simplex being optimized within the linear program. If a viable solution to the linear program in (28) can be found, then it is known that $\mathbf{y} \in \mathcal{M}_N$. Therefore, we empirically solve for the vectors \mathbf{y} and $(\boldsymbol{\Phi}_i)_{i=1}^N$ using the two-layer neural network after each epoch and use the `linprog` package in SciPy to determine whether (28) is solvable, thus allowing us to determine when $\mathbf{y} \in \mathcal{M}_N$.

In our actual implementation, we slightly modify the linear program in (28) to account for the fact that our two-layer neural network is trained with a sigmoid activation on the output neuron. Namely, one can observe that for targets of one, the neural network output can be considered correct if the output value is greater than zero and vice versa. We formulate the following linear program to better reflect this correct classification behavior:

$$\begin{aligned}
& \min \mathbf{c}^\top \boldsymbol{\alpha} & (29) \\
& \text{such that } A\boldsymbol{\alpha} < \mathbf{0} \\
& B\boldsymbol{\alpha} > \mathbf{0} \\
& Z\boldsymbol{\alpha} = \mathbf{1} \\
& \boldsymbol{\alpha} \geq \mathbf{0}
\end{aligned}$$

⁹Experiments are repeated with multiple learning rates and the best results are reported.

where $A \in \mathbb{R}^{\frac{m}{2} \times N}$ is a matrix of feature column vectors corresponding to a label of zero, $B \in \mathbb{R}^{\frac{m}{2} \times N}$ is a matrix of feature column vectors corresponding to a label of one, and other variables are defined as in (28). In words, (29) is solvable whenever a simplex can be found to re-weight neuron outputs such that the correct classification is produced for all examples in the dataset. The formulation in (29) better determines whether $\mathbf{y} \in \mathcal{M}_N$ given the modification of our two-layer neural network to solve a binary classification problem.

C Experimental Details

C.1 MLP Experiments

We first provide a clear algorithmic description of the pruning algorithm used within all MLP experiments. This algorithm closely reflects the update rule provided in (7). However, instead of measuring loss over the full dataset to perform greedy forward selection, we perform selection with respect to the loss over a single mini-batch to improve the efficiency of the pruning algorithm. We use $f(\Theta, \mathbf{X}')$ to denote the output of a MLP network with parameters Θ over the mini-batch \mathbf{X}' and $f_{\mathcal{S}}(\Theta, \mathbf{X}')$ to denote the same output only considering the neuron indices included within the set \mathcal{S} . Notice that a single neuron can be selected more than once during pruning.

Algorithm 1: Greedy Forward Selection for Two-Layer MLP

N := hidden size; P := pruned size; \mathcal{D} := training dataset

Θ := weights; $\Theta^* = \emptyset$

$i = 0$

while $i < P$ **do**

$j = 0$

$\text{best_idx} = -1$

$\mathcal{L}^* = \infty$

$\mathbf{X}', \mathbf{y}' \sim \mathcal{D}$

while $j < N$ **do**

$\mathcal{L}_j = \frac{1}{2} (f_{(\Theta^* \cup j)}(\mathbf{X}') - \mathbf{y}')^2$

if $\mathcal{L}_j < \mathcal{L}^*$ **then**

$\mathcal{L}^* = \mathcal{L}_j$

$\text{best_idx} = j$

end

$j = j + 1$

end

$\Theta^* = \Theta^* \cup \text{best_idx}$

$i = i + 1$

end

return Θ^*

We present in-depth details regarding the hyperparameters that were selected for the MLP experiments in the main text. To determine the optimal learning rate and number of pre-training iterations, we adopt the same setup as described in the MLP Experiments section in the main text and train MLP models of various sizes with numerous different learning rates. These experiments are then replicated across several different sub-dataset sizes. The results of these experiments are shown in Fig. 4. From these results, it can be seen that the optimal learning rate does not change with the size of the dataset, but it does depend on the size of the MLP. Namely, for MLPs with 5K or 10K hidden neurons the optimal learning rate is 1e-5, while for MLPs with 20K hidden neurons the optimal learning rate is 1e-6. It can also be seen in Fig. 4 that models converge in roughly 8000 training iterations for all experimental settings, which leads us to adopt this amount of pre-training in the main experiments.

To determine the optimal pruned model size, we first fully pre-train MLP models of different hidden sizes (i.e., $N \in \{5K, 10K, 20K\}$) over the full, binarized MNIST dataset. Then, these models are pruned to different hidden neuron sizes between 1 and 500. At each possible hidden dimension for the pruned model, we measure the performance of the pruned model over the entire training dataset. The results of this experiment are depicted in Figure 5. As can be seen, the accuracy of the pruned models plateaus at a hidden dimension of 200 (roughly). As a result, we adopt a size of 200 neurons as our pruned model size within all MLP experiments.

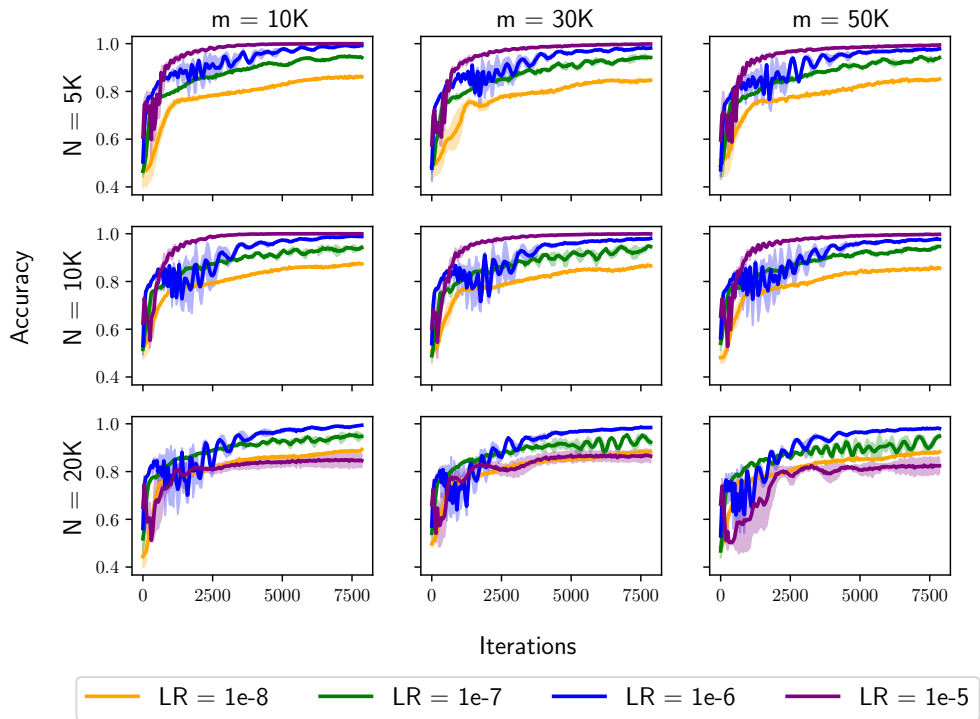


Figure 4: Training accuracy of two-layer MLP models on binarized versions of MNIST as described in the MLP Experiments Section in the main text. Different subplots display results for several different learning rates for models trained with different settings of m and N (i.e., dataset size and number of hidden neurons, respectively). Shaded regions represent standard deviations of results, recorded across three separate trials.

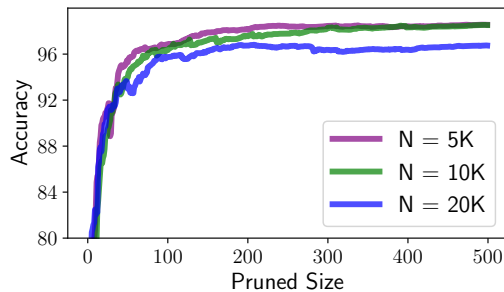


Figure 5: The performance of MLP models of different hidden dimensions over the entire, binarized MNIST dataset that have been pruned to various different hidden dimensions.

C.2 CNN Experiments

We begin with an in-depth algorithmic description of the greedy forward selection algorithm that was used for structured, channel-based pruning of multi-layer CNN architectures. This algorithm is identical to the greedy forward selection algorithm adopted in [65]. In this algorithm, we denote the weights of the deep network as Θ , and reference the weights within layer i of the network as Θ_i . Similarly, we use $\Theta_{\ell:}$ to denote the weights of all layers following layer ℓ and $\Theta_{:\ell}$ to denote the weights of all layers up to and including layer ℓ . C denotes a list of hidden sizes within the network, where C_ℓ denotes the number of channels within layer ℓ of the CNN. Again, we use $f(\Theta, \mathbf{X}')$ to denote the output of a MLP network with parameters Θ over the mini-batch \mathbf{X}' and $f_S(\Theta, \mathbf{X}')$ to denote the same output only considering the channel indices included within the set S .

Algorithm 2: Greedy Forward Selection for Deep CNN

C := hidden sizes; ϵ := stopping criterion; \mathcal{D} := training dataset

Θ := weights; L := # Layers; $\Theta_\ell^* = \emptyset \quad \forall \ell \in [L]$

$\ell = 0$

while $\ell < L$ **do**

while *convergence criterion is not met* **do**

$j = 0$

$\text{best_idx} = -1$

$\mathcal{L}^* = \infty$

$\mathbf{X}', \mathbf{y}' \sim \mathcal{D}$

while $j < C_\ell$ **do**

$\Theta' = \Theta^* \cup \Theta_{\ell:} \cup (\Theta_\ell^* \cup j)$

$\mathcal{L}_{\ell,j} = \frac{1}{2} (f_{\Theta'}(\mathbf{X}') - \mathbf{y}')^2$

if $\mathcal{L}_{\ell,j} < \mathcal{L}^*$ **then**

$\mathcal{L}^* = \mathcal{L}_{\ell,j}$

$\text{best_idx} = j$

end

$j = j + 1$

end

$\Theta_\ell^* = \Theta_\ell^* \cup \text{best_idx}$

end

$\ell = \ell + 1$

end

return Θ^*

Now, we present more details regarding the hyperparameters that were utilized within large-scale experiments. For ImageNet experiments, we adopt the settings of [65].¹⁰ For CIFAR10, however, we tune both the setting of ϵ and the initial learning rate for fine-tuning using a grid search for both MobileNetV2 and ResNet34 architectures. This grid search is performed using the full CIFAR10 dataset instead of some sub-dataset. The results of this grid search are shown in Figure 6. As can be seen, for MobileNetV2, the best results are achieved using a setting of $\epsilon = 0.02$, which results in a subnetwork with 60% of the FLOPS of the dense model. Furthermore, an initial learning rate of 0.01 yields consistent subnetwork performance for MobileNetV2. For ResNet34, a setting of $\epsilon = 0.05$ yields the best results and yields a subnetwork with 60% of the FLOPS of the dense model. Again, an initial learning rate of 0.01 for fine-tuning yields the best results for ResNet34. For the rest of the hyperparameters used within CIFAR10 experiments (i.e., those used during pre-training), we adopt the settings of a widely-used, open-source repository that achieves good performance on CIFAR10 [40].

D Better Aligning Theory and Practice

Here, we discuss the pruning methodology used within our work in comparison to [65]. For ease, we replicate several definitions that are included in the main text. The greedy forward selection strategy

¹⁰We adopt all of the same experimental settings, but decrease the number of fine-tuning epochs from 150 to 80 because we find that testing accuracy reaches a plateau well-before 150 epochs.

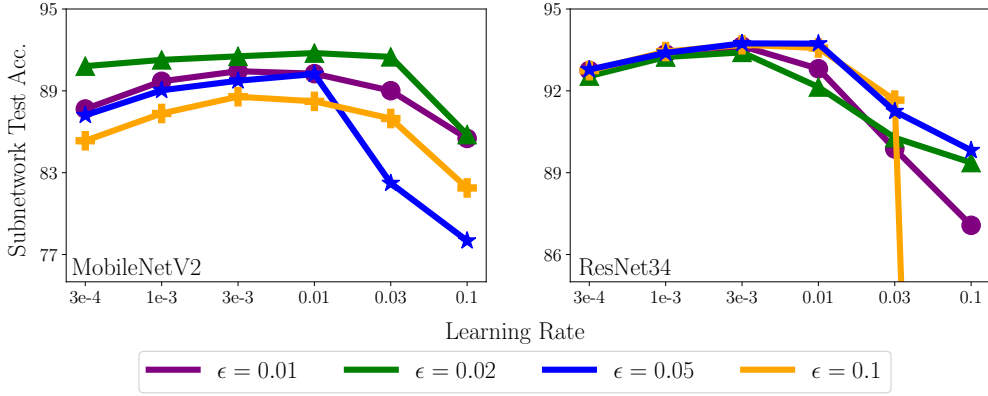


Figure 6: Subnetwork test accuracy on the CIFAR10 dataset for different settings of ϵ and initial learning rate for fine-tuning. All models are pre-trained identically for 200 epochs. Fine-tuning is performed for 80 epochs, and we report test accuracy for each subnetwork at the end of fine-tuning.

used for pruning in both our work and [65] can be summarized by the equation below.

$$\mathcal{S}_{t+1} = \mathcal{S}_t \cup i^*, \text{ where } i^* = \arg \min_{i \in [N]} \mathcal{L}[f_{\mathcal{S}_t \cup i}]$$

This greedy forward selection algorithm finds an approximate solution to the difficult combinatorial optimization problem shown below.

$$\mathcal{S}^* = \arg \min_{\mathcal{S} \in [N]} [f_{\mathcal{S}}], \quad |\mathcal{S}^*| \ll N$$

In practice, this pruning methodology is extended to deeper networks by applying forward selection in a greedy layer-wise fashion over every layer of the network, beginning from the first layer. To analyze the performance of greedy forward selection from a theoretical perspective, we consider two-layer neural networks of width N and adopt the analytical formulation given by the following equations.

$$\mathbf{u}_k = \frac{1}{k} \cdot \mathbf{z}_k, \quad \mathbf{z}_k = \mathbf{z}_{k-1} + \mathbf{q}_k, \quad \mathbf{q}_k = \arg \min_{\mathbf{q} \in \text{vert}(\mathcal{M}_n)} \ell \left(\frac{1}{k} \cdot (\mathbf{z}_{k-1} + \mathbf{q}) \right)$$

The benefits of this formulation are twofold: (i) it allows the loss of the pruned network to be easily compared to the loss of the original network and (ii) it exactly matches the pruning algorithm used in practice. In comparison, [65] also consider wide, two-layer neural networks, but use the pruning formulation outlined below.

$$\mathbf{u}_k = (1 - \varepsilon_k) \mathbf{u}_{k-1} + \varepsilon_k \mathbf{q}_k, \quad \mathbf{q}_k = \arg \min_{\mathbf{q} \in \text{vert}(\mathcal{M}_n)} \ell \left((1 - \varepsilon_k) \mathbf{u}_{k-1} + \varepsilon_k \mathbf{q} \right)$$

The update strategy shown above yields a close resemblance to the Frank-Wolfe algorithm [34]. However, this formulation does not match the pruning algorithm used in practice. Namely, there is no notion of a step size ε_k within the greedy forward selection algorithm. Rather, the greedy forward selection algorithm maintains a growing subset of neurons, sampled from the full network, and constructs a pruned network by performing a forward pass with only this subset of neurons. We formulate this pattern exactly within our analysis in an attempt to provide a more realistic theoretical understanding of the empirical performance of greedy forward selection.